Université de Montréal

Thermoresponsive Porous Hydrogels :

Synthesis, Characterization and Potential Applications

par

Sumitra Rajagopalan

Département de Chimie

Faculté des études supériures

Mémoire presenté à la faculté des études supériures en vue de l'obtention du grade de Maître ès sciences (M.Sc) en Chimie

Août 2001

Université de Montréal

Faculté des études supériures

Ce mémoire intitulé

Thermoresponsive Porous Hydrogels :

Synthesis, Characterization and Potential Applications

Présenté par:

Sumitra Rajagopalan

A été évalué par un jury composé des personnes suivants:

Professor Tom Ellis	président du jury
Professor Julian Zhu	directeur de recherche
Professor Antonella Badia	membre du jury

Mémoire accepté le: .....

He whose doings are not motivated by selfish ends or desire for results, whose actions are driven by the thirst for knowledge, he is the one the Sages call Buddha – the Wise One.

Chapter 3, Verse 35
The Bhagavad Gita

Résumé

Cet étude porte sur les aspects théoriques et practiques des hydrogels thermosensibles et poreux à base de poly(*N,N*-diethylacrylamide). Des gels thermosensibles et poreux ont eté synthétisés en utilisant le principe de séparation des phases. Nous avons réussi à induire une séparation des phases au niveau microscopique pendant le processus de gelification, en variant la température de la réaction et le taux de réticulation. Les hydrogels poreux obtenus par variation de température (temperature-induced phase separation) ont un taux de gonflement plus élevé que ceux obtenus en variant la concentration du monomère réticulant. Nous avons observés une relation entre le taux de gonflement et la microstructure. Des images obtenues par la microscopie optique demontrent l'existence de pores dans les gels obtenus par la séparation des phases. Avec l'aide des données d'absorption d'eau et également des mesures de transmittance de la lumière, un modèle qualitatif décrivant le rapport entre les conditions de gelification et la microstructure a été proposé. Les techniques spectrophotométriques et gravimétriques ont eté utilisées pour comparer les comportements physicochimiques à une température critique (LCST – lower critical solution temperature) des gels non-poreux et de ceux poreux. Les gels poreux n'éprouvent pas de changement brusque d'opacité à l'LCST – comportement typique des gels thermosensibles et non-poreux. Par contre, nous avons observé un changement de volume beaucoup plus brusque dans le cas des gels thermosensibles et poreux qu'avec des gels conventionnels. Ces observations nous ont permis de proposer un modèle qualitatif pour interpréter le phénomène de l'LCST dans les gels poreux et non-poreux. Finalement, afin de démontrer l'utilité de ces gels, nous avons utilisé les gels thermosensibles et poreux afin de préparer des matériaux à mémoire de forme et des systèmes mécanochimiques.

Mots clés *: hydrogels thermosensibles, taux de gonflement, LCST, porosité, séparation de phases.*

Abstract

This study examines both the theoretical and practical aspects of porous, thermoresponsive hydrogels based on poly(*N,N*-diethylacrylamide). It has been confirmed that porous thermoresponsive hydrogels can be induced through simultaneous phase separation and crosslinking, by carrying out the gelation reaction, in part or in whole, above the lower critical solution temperature (LCST). We have also devised a method of synthesizing porous thermoresponsive hydrogels through crosslinking-induced phase separation (CLIPS). The porous hydrogels synthesized through temperature-induced phase separation displayed improved water absorption capacity over their non-porous counterparts, while the porous hydrogels prepared through CLIPS exhibited lower swelling ratios. Images obtained through inverted optical microscopy show clearly the presence of pores in the phase-separated gels. Gravimetric and spectrophotometric techniques were used to compare the phase transition behavior of thermoresponsive porous hydrogels with conventional thermoresponsive hydrogels. The thermoresponsive porous hydrogels exhibited a unique phase transition behavior at the LCST. Unlike conventional hydrogels which undergo an abrupt decrease in light transmittance around the LCST, porous hydrogels show no abrupt increase in opacity. However, the shrinking capacity of these porous thermoresponsive hydrogels, above their LCST, was found to be significantly larger than that of conventional hydrogels. Based on these observations, a conceptual model describing the phase-transition process in both conventional and phase-separated hydrogels was developed. To demonstrate the potential applications of thermoresponsive porous hydrogels, we have created thermosensitive shape-memory materials and artificial muscles.

***Keywords**: thermoresponsive hydrogels, LCST, swelling ratio, porosity, microphase separation.*

Table of Contents

List of Figures

List of Tables

List of abbreviations

AFM:	Atomic Force Microscopy
CLIPS:	Crosslinking-induced Phase Separation
C_{sh}:	Shrinking Capacity
HPC:	Hydroxypropyl Cellulose
IPN:	Interpenetrating Network
LCST:	Lower Critical Solution Temperature
LSCM:	Laser Scanning Confocal Microscopy
MBA:	Methylene-bis acrylamide
MPS:	Microphase separation
PDEA:	Poly (*N,N*-diethylacrylamide)
PEG:	Poly(ethylene glycol)
PNIPAM:	Poly(*N*-isopropylacrylamide)
PVME:	Poly(vinyl methyl ether)
SEM:	Scanning Electron Micrography
SMM:	Shape-Memory Materials
SR:	Swelling Ratio
TEMED:	Tetramethylethylene diamine
TIPS:	Temperature-Induced Phase Separation
W_d:	Weight of Dry Gel
W_{sh}:	Weight of Shrunk Gel
W_{sw}:	Weight of Swollen Gel

Acknowledgements

I would first like to express my profound gratitude to my thesis supervisor, Professor Julian Zhu. His warm and friendly disposition helped create a congenial work environment while his meticulous approach and eye for the smallest details ensured that I put in my best into this thesis. The knowledge and skills gained under his guidance will keep me in good stead as I move on to pursue doctoral studies and a career in research.

I would like to thank the members of our research group. I thank David and Mohand for having synthesized the monomer as well as Wilms and Damien for their ideas and suggestions. I thank all the others – Laurent, Zhengji, Qiang and Ernesto for contributing to a pleasant working environment.

I appreciate the professors in our department for being ever so helpful and supportive. I am particularly grateful to Professors Jacques Prud'homme, Michel Lafleur and Antonella Badia for having provided me with helpful suggestions. I would also like to thank Professor Gilles Durocher for having kindly allowed us to use his spectrophotometric instrument for analysis.

I would like to take this opportunity to thank those who introduced me to the fascinating world of polymer science. I am indebted to Professor Alexander Y. Bilibin of St. Petersburg State University, whose introductory course on macromolecular chemistry inspired me to specialize in polymers. I also owe a debt of gratitude to Professor Konstantin Makarov of the Pavlov Medical Academy in St. Petersburg for my first hands-on experience in a polymer science laboratory.

Finally, I would like to thank my parents whose material and moral support have allowed me to pursue my graduate studies in Montreal and my brother Vikram for keeping me in good spirits. Last but not least, I would like to pay homage to the teachings of the *Bhagavad Gita* – our sacred text, whose words of wisdom are as relevant today, as they were more than 2000 years ago.

To my parents,

To Professor Alexander Y. Bilibin

1. Introduction

1.1 Stimuli-Responsive Hydrogels

Stimuli-responsive or "smart" materials have been an active area of research work in recent times [1-2]. Research efforts have been focused on developing a new generation of materials and composites that not only possesses the desirable mechanical properties and texture, but are also able to react in a specific manner to a specific environmental stimulus. By definition, stimuli-sensitive materials are those materials that have the capability to select and execute specific functions in response to changes in environmental stimuli. Research groups around the world are working on a wide variety of stimuli-sensitive materials ranging from ferroelectric fluids, metal alloys, piezoelectric materials and polymers.

Of such stimuli-responsive materials, stimuli-responsive hydrogels have been an area of active research in recent years [3-18]. Hydrogels are three-dimensional crosslinked polymer networks swollen in water. Owing to a delicate balance of opposing forces that coexist in such a system, gels have a remarkable ability to interconvert between two phases - that of a completely swollen phase and a collapsed one (Figure 1.1). More recent work has pointed to the existence of multiple phases in gels [4]. The collapse of hydrogels can be brought about by small changes in temperature [5], pH [6], electric field [7], magnetic field [8] or even a molecular stimulus like antigens [9] or metal ions [10].

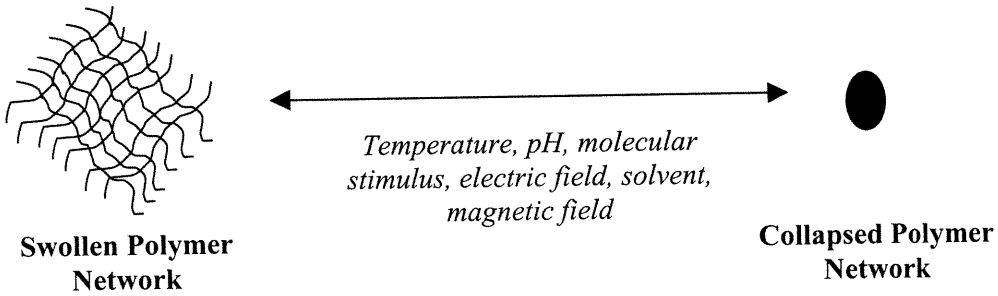

Figure 1.1 Stimuli-induced collapse and recovery of hydrogels

Such a collapse manifests itself in many ways from molecular and supramolecular reorganization to changes in macroscopic properties like turbidity and volume change.

In a report on stimuli-responsive hydrogels in 1997 [11], a survey of the latest trends and developments in the field over the last two decades was made. According to this report, stimuli-responsive hydrogels caught the attention of scientists back in 1975 when T. Tanaka of the Massachusetts Institute of Technology observed an abrupt change in turbidity in polyacrylamide gels on increasing the acetone concentration. The observation of this phase transition phenomenon spurred an intense interest in the field, both to understand the fascinating chemistry of stimuli-sensitive hydrogels, and to explore their potential application in areas as diverse as biomedicine and robotics.

It was later discovered that all hydrogels could undergo a discontinuous phase transition by simply applying a specific environmental stimulus that would provoke a collapse of the gel. Of the many applications suggested were the use of hydrogels for stimuli-induced binding and release of entrapped molecules, including drugs. Other applications include artificial muscles for robotic applications, chemical memories, molecular separation systems and toys.

Studies on stimuli-responsive hydrogels abound. Amongst the more fascinating results reported are electroactive polymer hydrogels [12], that could be potentially used as artificial muscles, hydrogels that shrink to almost 1000 times their size with a slight change in pH [13] and hydrogels that can shrink and release their contents under the influence of a biochemical stimulus like glucose [14].

Other work includes shape-memory materials [15], drug-delivery devices [16] and separation agents based on stimuli-responsive hydrogels [17]. All in all, the results reported so far point to the many exciting potential applications of hydrogels, while at the same time highlighting the need for further fundamental research in order to better exploit their fascinating properties.

1.2 Thermosensitive Polymers and Gels

Of all the stimuli-sensitive hydrogels described above, thermoresponsive or thermosensitive hydrogels are, by far, the most widely studied [5-18]. As mentioned earlier, a delicate balance of opposing forces coexist in a hydrogel and an external stimulus capable of tilting this balance will cause the gel to shrink. In the case of thermosensitive hydrogels, their monomeric units contain a delicate balance of hydrophobic and hydrophilic moieties. Low temperatures favour hydrophilic interactions, through hydrogen bonding with the surrounding water molecules, whereas higher temperatures above the LCST cause the rupture of these hydrogen bonds, thus leading to intramolecular rearrangement and aggregation of the polymeric side chains through hydrophobic interactions. This aggregation of polymer chains provokes a collapse in the case of hydrogels and precipitation in the case of linear polymers in aqueous solution. The temperature at which this transition from swollen to collapsed state takes place is known as *lower critical solution temperature* (LCST). Some examples of common thermosensitive polymers include poly(*N*-isopropylacrylamide), poly(*N,N*-diethylacrylamide), poly(hydroxypropyl cellulose), poly(vinyl methyl ether) and poly(ethylene oxide) (Figure 1.2).

Amongst the thermosensitive hydrogels known so far, poly(*N*-isopropylacrylamide (PNIPAM), has received the maximum attention, partly due to its sharp phase transition and the fact that it has a LCST at around 37°C, which is close to the normal temperature of the human body. It was believed that hydrogels based on PNIPAM could be used as drug delivery vehicles. While an exhaustive review of all the work done on thermosensitive polymers and hydrogels is beyond the scope of this thesis, we will provide a brief overview of the strides made in the field to date.

The literature abounds with work on PNIPAM. To summarize all the results produced by research groups in fields as diverse as chemistry, physics and bioengineering as well as to smooth out redundancies and contradictory results, H.G Schild of IBM Corp. published a review in *Progress in Polymer Science* [18]. He provided a comprehensive overview of both the fundamental and applied aspects of thermosensitive polymers and hydrogels. He first surveyed all the polymerization

techniques used to create PNIPAM linear polymer and gels, including solution polymerization, suspension polymerization, radiation-induced polymerization and photoinitiated polymerization. He also examined the work done in further functionalizing thermosensitive polymers through copolymerization or grafting of other molecules onto the backbone. The review also provided a comprehensive overview of all the possible applications of PNIPAM polymers and hydrogels and of other thermosensitive polymers in general. This included drug delivery vehicles, agents for bioseparations, reversible absorbents, artificial muscles and actuators.

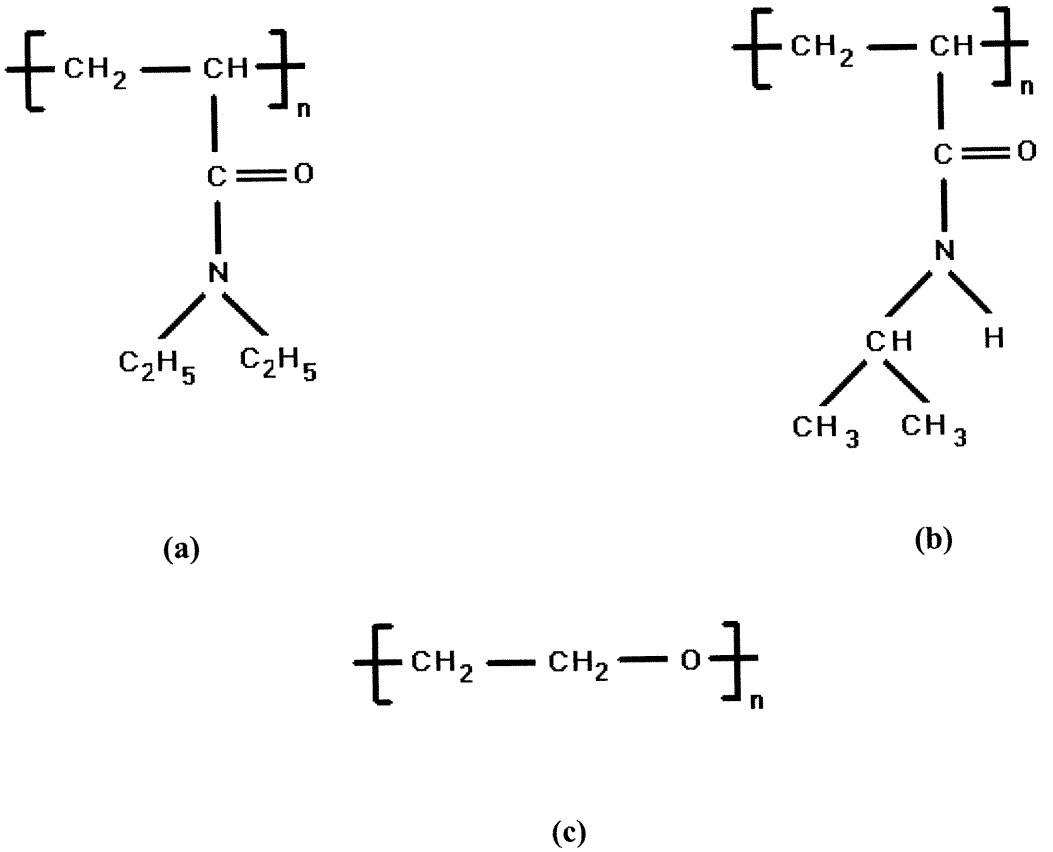

Figure 1.2 Some common thermosensitive polymers. (a) poly(*N,N*-diethylacrylamide) ; (b) poly(*N* -isopropylacrylamide); (c) poly(ethylene glycol).

The LCST phenomenon remains a focus of research efforts and, to date, no universally-accepted interpretation of this critical phenomenon exists. Some of the researchers base their model on the Flory-Huggins theory of solutions [19], while

others resort to the lattice-fluid-hydrogen-bond theory [20], which takes both hydrophobic and hydrophilic interactions into account. Also, the literature presents highly polarized views on the role of hydrogen-bonding during the phase-transition. Some researchers insist the rupture of hydrogen bonds causes an aggregation of the polymer side chains while others maintain that the phase transition is only a result of hydrophobic interactions. Researchers have used a variety of experimental tools to come up with a model that can adequately describe the phenomenon. Differential scanning calorimetry [21] has been used to measure the endotherm associated with the phase transition, while UV-visible spectrophotometry affords a measure of the cloud point of the polymer which corresponds to the LCST [22]. Light scattering techniques have been used to monitor the change in the radius of gyration of the polymer chains upon aggregation [23]. Nuclear magnetic resonance spectroscopy has been used to study the change in relaxation time of the various protons during the phase transition [24], while infrared spectroscopy has been used to observe molecular level changes at the LCST [25]. While the interpretation of these results vary, the general consensus is a coil-to-globule transition of the chains that occurs at the LCST owing to the breaking of hydrogen bonds with the surrounding water molecules followed by aggregation of the hydrophobic lateral chains of the polymer networks. A summary of these techniques is given in Table 1.1.

Clearly, a lot more work is needed to fully understand the LCST phenomenon and to smooth out the contradictions found in the literature. As part of our work on thermoresponsive gels, we have proposed a simple model to describe the phase transition of conventional hydrogels versus porous hydrogels. Details can be found in Section 3.2.1.

Many authors have further pursued their study of thermosensitive polymers and hydrogels [26-45]. Some have studied the effect of copolymerizing thermosensitive polymers with more hydrophilic or hydrophobic monomers [26-30]. As expected, the presence of hydrophilic moieties in the polymer caused an increase in its solubility and hence an increase in the LCST. The effect of the hydrophobic comonomers was reverse. The effect of ionic comonomers was also discussed. While many reported a more discontinuous or abrupt phase transition in the case of such

Table 1.1. Common experimental methods used to determine the LCST

Method	Parameter Measured
Visible spectrophotometry/ turbidimetry	Cloud point – temperature at which solution/ gel turns opaque
Differential scanning calorimetry	Enthalpy change at LCST
Nuclear magnetic resonance	Changes in relaxation times of the backbone and side-chain protons at LCST
Infrared spectroscopy	Frequency shifts of certain characteristic peaks at LCST
Flourescense spectroscopy	Change in the intensity of fluorescent probe molecule at LCST
Rheometry	Change in the flow properties at LCST
Light scattering	Change of the radius of gyration at LCST
Gravimetry/ volumetry	Weight change/volume change at LCST
Atomic force microscopy	Appearance of domain-like structures at LCST
Raman microscopy	Appearance of domain-like structures at LCST
Viscosimetry	Change in the viscosity of the polymer solution at LCST

polymers, there are reports pointing to the contrary. A universally accepted view is yet to emerge. While many researchers have concentrated their efforts towards modifying the properties of thermosensitive polymers through copolymerization, few

research groups are working on the synthesis of new monomers that would form thermosensitve polymers. In one such study [31], α–alkyl substituted acrylates that possess an LCST, were synthesized.

There are currently a handful of research groups working on thermosensitive interpenetrating networks (IPNs) [32-34]. IPNs are gels consisting of two or more networks embedded in each other (Figure 1.3). Though there are very few references available, the work carried out so far points to IPNs having rather unusual thermosensitive properties. Byrin *et al.* were able to synthesize thermosensitive IPNs based on polyacrylamide, poly(*N,N*-dimethylacrylamide) and poly(acrylic acid) [32], polymers that are otherwise hydrophilic and do not display any thermosensitive properties. In this case, a step-wise, rather than an abrupt decrease in swelling ratio, is observed on heating the gel. Similarly, another study involved synthesizing thermosensitive IPNs based on poly(vinyl alcohol) with poly(acrylic acid) [33]. Here, a step-wise change in the swelling ratio of the gel as a function of temperature was observed. Depending on the composition of the IPN, either an increase or decrease was observed. In the case of conventional thermosensitive hydrogels, one usually observes an increase in the LCST on adding hydrophilic moieties to the system. In the case of the thermosensitive semi-IPNs prepared by Shin *et al.* [34], the reverse was observed. Addition of linear hydrophilic chains caused a decrease in the LCST. This was attributed to the fact that the hydrophilic chains were involved in hydrogen bonding with the network and were thus protected from exposure to water. This apparently increased the hydrophobicity of the network and hence caused a decrease in the LCST.

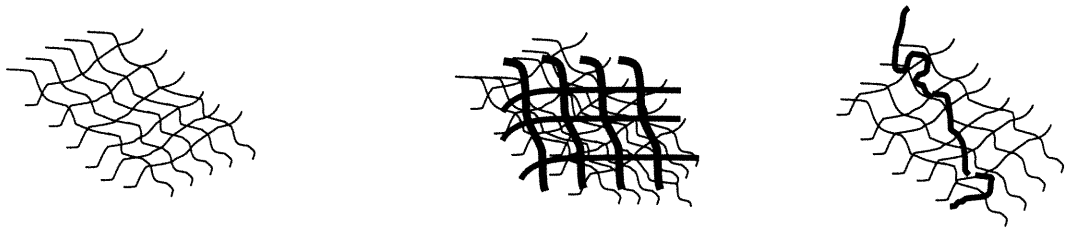

Figure 1.3 Model of (a) conventional polymer network (b) interpenetrating polymer network (IPN) and (c) semi-interpenetrating polymer network.

Thermosensitive polymers and hydrogels have been one of the main research areas in our laboratory. So far, we have explored the effect of hydrophilic and hydrophobic comonomers on the LCST of a thermosensitive polymer [35], designed membrane immobilization systems using thermosensitive polymers [36] and studied the diffusion of select solute molecules in thermosensitive polymer matrix [37]. Current work includes combining thermosensitive polymers with biocompatible bile-acid moieties to create biomedical thermosensitive polymers. We are also working on reversible absorbents based on thermosensitive polymers. Thermal and rheological methods have been used to study thermosensitive polymers in solution as well as hydrogels. A novel FTIR technique to determine the LCST of linear polymers and hydrogels was developed [38]. We are currently exploring the use of thermosensitive polymers to selectively recover certain metal ions from industrial wastes. We have focussed much of our research efforts on polymers and hydrogels based on *N,N*-diethylacrylamide which has not received as much attention in the literature as PNIPAM.

1.3 Swelling / Dehydration Kinetics in Hydrogels

The kinetics of swelling and dehydration of thermosensitive hydrogels have been the focus of many researchers [39-42]. Preliminary research work carried out in our laboratory highlighted the need to develop fast-response hydrogels. Indeed, most of our applications centred on the ability of thermosensitive hydrogels to quickly recover and release encapsulated substances, be it drugs, waste products or physiological fluids. As already mentioned in the literature, swelling and deswelling kinetics remains a major obstacle to commercializing hydrogel-based technologies. We thus decided to explore ways and means to improve the response time in thermosensitive hydrogels. We also noticed, even after an exhaustive literature search, that there exists no mathematical parameter that could quantify the extent a hydrogel can collapse under the influence of the external stimulus. This could be a parameter that would be used to estimate the extent a thermosensitive hydrogel could collapse above the LCST and recover its original conformation upon cooling.

Various methods to improve the kinetics of swelling and dehydration were proposed by research groups working on hydrogels. The most obvious technique was to reduce the size of the gel [43]. The response time of environmentally-sensitive gels can be dramatically reduced by decreasing the characteristic diffusion path length, since time scales with the square of the dimension for a diffusion-limited process. However, small gels or microgels are unsuitable for a range of applications. Other suggestions involved incorporating hydrophilic polymer chains [44] into the thermosensitive polymer network, that would act as a water channel and thus accelerate the swelling process.

Kaneko *et al.* proposed a novel approach [45]. They designed comb-type grafted thermosensitive hydrogels through the polymerization of N-isopropylacrylamide with a PNIPAM macromonomer. These new thermosensitive copolymers displayed higher equilibrium swelling at lower temperatures and rapid deswelling kinetics at elevated temperatures as compared to conventional cross-linked thermosensitive polymers.

The most common method for improving swelling kinetics, however, is the creation of a porous microstructure in the hydrogel. This involved creating a network of interconnected pores throughout the gel. The theory behind this was that water uptake and release would occur through capillary action, through the seeping of water through its pores, rather than slow diffusion through a non-porous material.

1.4 Porous Hydrogels

Several methods have been devised to create porous hydrogels. One of the most common techniques is freeze-drying of gels [46-48]. In this method, the gel is rapidly cooled in liquid nitrogen and the frozen gel is dried under low pressure and temperature. During this process, the mesh-size inside the gel increases due to water expansion. Thereafter, at low temperature and pressure, the ice sublimes into water vapour which is then expelled from the gel matrix leaving behind voids or pores. This is the method used by Kato *et al.* [47] to create macroporous hydrogels as well as by Hu *et al.* to create inhomogeneous poly(acrylonitrile-co-acrylamide-co-acrylic acid) hydrogels [48].

Another method used by Apple *et al.* is the technique of inverse suspension polymerization whereby the aqueous reaction mixture consisting of monomer, initiator and crosslinker was dispersed in a poor solvent [49]. The gel was then dried at a temperature above the boiling point of the poor solvent which left voids in the matrix. A similar technique involves the polymerization of microemulsions containing different alkyl chain lengths of cationic surfactants. In this method, devised by Chieng *et al.* of the University of Singapore, photoinitiated polymerization was carried out on bicontinuous microemulsion samples to form microporous materials [50]. The morphology of the microporous polymeric solids showed a drastic change from worm-like to oval-shaped to globular structures on decreasing the alkyl chain length of the surfactant. These polymeric materials possessed an open-cell structure.

Macroporous gels are of interest to research groups working on gel electrophoresis. In the latter, polyacrylamide and agarose are the gels of choice as a medium for separations. It goes without saying that separation and recovery of macromolecules can be facilitated by the presence of pores. P. Righetti of the University of Milan [51] presented a comprehensive review on the techniques used to create macroporous gels for electrophoresis. He described two techniques, polymer-induced lateral aggregation and temperature-induced lateral aggregation. In the former, pores were created by increasing crosslinker concentration while in the latter, pore formation was brought about by decreasing the temperature. He interpreted the above as the bundling or aggregation of polymer chains under such conditions which, in turn, creates voids or pores.

Porous hydrogels are also widely used in chromatography. Terauchi of Nippon Paints prepared hydrophilic and durable porous particles based on 2,3-dihydroxypropyl methacrylate monomer, through suspension polymerization using chlorobenzene as the inert solvent and poly(vinyl alcohol) (PVA) as a stabilizer [52]. The pore radius was controlled through the volume of porogen added. In this case, chlorobenzene served as the porogen as it created voids in the gel on evaporation. Scanning electron micrography (SEM) images revealed a porous interconnected

structure. The gel particles so obtained were found to be suitable for chromatographic applications.

Using a freeze-thaw technique, cellular PVA hydrogels were prepared [53]. A concentrated aqueous solution of PVA was subjected to a freeze-thaw cycle until a gel was formed. This technique not only created porous structures but also improved the mechanical strength of the hydrogels. Swelling kinetics improved dramatically as a result of the pores. Other pore-formation techniques simply involved modulating synthesis variables such as monomer or crosslinker concentration. Porous styrene/divinyl benzene resins [54] as well as porous polyacrylamide gels [55] have been prepared by the use of this method.

Superporous hydrogels with open channels have been synthesized using the gas-blowing or foaming technique [56]. The capillary radius of the porous hydrogels so obtained were in the range of a few hundred micrometers. The hydrogels obtained using this technique are also known as hydrogel foams. The foaming technique was carried out using a foaming agent ($NaHCO_3$) and a foam stabilizer. Gas bubbles were produced through the action of sodium bicarbonate with an acid. A surfactant (sodium dodecyl sulphate) was used as a foam stabilizer. In this process, timing was a critical factor, namely, the timing of the foam formation and the polymerization process. If the foaming started too early or the polymerization proceeded too slowly, the foam rose and subsided before the onset of gelation. On the other hand, if the foaming started too late, the solution became too viscous for the even distribution of gas bubbles. The SEM images of the dried gels clearly showed the presence of interconnected pores with sizes in the order of a few micrometers. The porosity increased as the amount of $NaHCO_3$, acid and foam stabilizer increased. The largest pore size of superporous hydrogels was calculated from the Young-Laplace equation. In addition, the effect of drying methods on the gel morphology was also investigated. The swelling kinetics of the hydrogels that were dried at 60^0C overnight, though faster than those of conventional hydrogels, was still too slow for the intended application. This was attributed to the fact that removal of water caused a collapse in polymer chains and hence the pores due to the high surface tension of water. On the other hand, the second method of drying, which involved dehydration in ethanol

before drying drastically, reduced the swelling time to about 4 minutes, thereby indicating the preservation of the gel morphology.

The biomaterials literature is replete with techniques to obtain macroporous hydrogels. Macroporous structures take on a special significance in biomaterials design. The presence of pores facilitates the integration of biomaterials with their physiological environment. The surrounding cellular bodies are able to invade the biomaterial through the pores thus facilitating its integration and minimizing inflammatory reactions in the body. In a paper on macroporous hydrogels for biomedical applications [57], the authors described two techniques used to create macroporous hydrogel membranes based on hydroxyethyl methacrylate – the freeze-thaw technique, already described above, and the porosigen technique, whereby a crystalline compound (sucrose) is dispersed in the monomer solution prior to polymerization. The influence of various comonomers was also discussed. SEM images of the gels revealed the presence of pores. Various applications of such gels including its use as a synthetic articular cartilage, as agents for separations and as substrates for cellular engineering were also discussed.

In another article, researchers reported the synthesis of a series of macroporous hydrogels through inverse suspension polymerization, combined with freeze-thaw techniques. These porous hydrogels were tested as hydrophilic substrates in hemoperfusion. The results showed that the pore size and surface area affect the leucocyte and blood platelet response [58].

Most of the techniques described above cannot be used to create pores in thermosensitive gels as the above requires the presence of a dispersed solvent. Thermosensitive polymers contain both hydrophilic and hydrophobic moieties and thus readily dissolve in both water and many common organic solvents. While the inverse suspension polymerization technique described above works well to create porous polymer beads, the same technique cannot be reproduced to create porous bulk gels. Other techniques like freeze-drying and foaming render the gels very fragile and would be unsuitable for many industrial and biomedical applications. Freeze-drying, though an effective method to induce pores, is not economically viable to be reproduced on an industrial scale.

1.5 Thermoresponsive Porous Hydrogels

The idea of exploiting the unusual solubility behaviour of thermoresponsive gels to create pores was formally put forward by S. Gehrke of the University of Cincinnati. The idea involved a process that would cause simultaneous crosslinking and phase separation to occur in order to create chemically crosslinked phase-segregated hydrogels (Figure 1.4). Their underlying hypothesis to create fast-response gels was that in the case of porous gels water uptake would occur through convection rather than through diffusion. Furthermore, the presence of channels between the pores would ensure continuous solvent flow throughout the gel. Interconnected pores, they hypothesized, would be brought about through spinodal decomposition into two bicontinuous microphases.

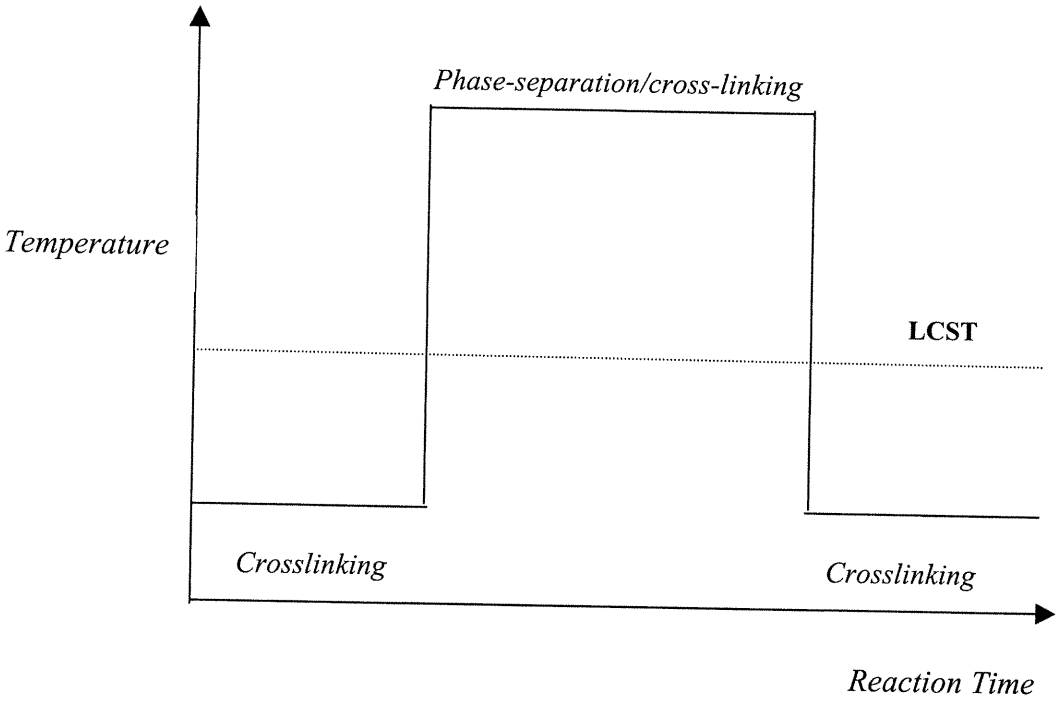

Figure 1.4 General scheme of a temperature-induced phase separation (TIPS) process in thermoresponsive hydrogels. The TIPS process involves carrying out a part of the gelation reaction at a specific temperature above the LCST.

In their first communication on this subject [59], they reported the synthesis of a fast-response cross-linked PNIPAM hydrogel whereby the pre-gel solution was heated to a temperature above its LCST to allow for phase separation during gelation, thus creating a phase-segregated structure whereby the polymer aggregates were locked in by crosslinks. Further work was carried out by the same group on other polymer systems using, what they coined, the temperature-induced phase separation (TIPS) method of creating porous structures in thermosensitive hydrogels.

Wu *et al.* further improved on the method proposed by Gehrke [60]. They synthesized porous poly(isopropylacrylamide) hydrogels by heating the solution above its LCST and at the same time using hydroxypropyl cellulose (HPC) as a nucleating agent. Upon heating the pre-gel solution, the HPC formed aggregates that enlarged the already existing pores. Using a similar approach, Yan and Hoffman [61] created porous thermosensitive hydrogels with pores large enough for the transport of macromolecules – in this case, a hydrogel with a macroporous structure to allow absorption of proteins plus rapid delivery in response to temperature change through LCST.

The most comprehensive study of temperature-induced phase separation (TIPS) process has been carried out by Kabra and Gehrke. In an article published in *Macromolecules*, the authors reported the design of porous, thermoresponsive hydroxypropyl cellulose gels [62]. A systematic study was carried out by modulating the time before phase separation (t_{BP}) and time during phase separation (t_{DP}). Interpretation of the results was based largely on the images obtained through SEM and measurements on effective porosity. By modulating t_{BP} and t_{DP}, it was concluded that by keeping the reaction time during phase separation long and the reaction time before phase separation short, one could obtain porous gels with an open-celled structure.

Further studies on simultaneous chemical gelation and phase separation were carried out with poly(vinyl methyl ether) (PVME), another thermosensitive hydrogel [63]. This time, gelation speed was introduced as a parameter and the crosslinking reaction was carried out through γ-radiation. Here, the size of the porous structure depends on the balance of the phase separation and gelation speed, which was

controlled by the radiation dose rate. The effect of a gradual temperature increase versus stepwise temperature jumps was also investigated. The images of the gels revealed a porous structure. It was therefore shown that γ-radiation could be used to induce porosity in the gel.

Similar work was carried out Gotoh *et al.* [64]. They reported the synthesis of porous thermoresponsive PNIPAM and PDEA gels. The results obtained here differ markedly from those of other authors. For one, the authors claimed that the gels obtained for PNIPAM were opaque, even when synthesized at 20°C, thereby suggesting that such gels have a phase-separated structure under any conditions. The results reported in this paper contradict most of the other results obtained so far. We have attempted to explain this contradiction in Section 3.2.1.

This microphase-separation technique has also been used to create porous hydrogel fibres that could be used as artificial muscles [65].

1.6 Characterization of Thermosensitive Porous Hydrogels

Various classical techniques to determine porosity already exist, like mercury intrusion and BET gas absorption. However, with porous hydrogels, the situation is rather different. Drying of gels often leads to collapse of the gel structure, and hence, these classical techniques are not applicable. Ideally, the hydrogel microstructure should be probed in its swollen state. Therefore, other methods need to be explored.

So far, three methods that allow for non-invasive imaging of porous thermoresponsive hydrogels in their swollen state have been reported. One of them is Raman microspectroscopy [49]. In this technique, an Argon laser at 488 nm was used to illuminate a macroporous hydrogel PNIPAM and the Raman spectra were recorded at various points (every 2 μm) on the sample along all three dimensions. The area of the peak corresponding to the CH_2 bending vibration at 1445 cm^{-1} was mapped as a function of position. Regions of minimal polymer concentration were taken to be pores. A three-dimensional map of the sample can show the presence of interconnected pores in the hydrogel.

Another equally effective technique is laser scanning confocal microscopy (LSCM) [66]. In this technique, fluorescence probes were added to the

thermosensitive hydrogel and an image of the internal structure of the gel was obtained using both reflection and fluorescence modes. Interpretation of the images was based on the contrast of bright and dark areas produced as a result of migration of the fluorescence probes towards the hydrophobic domains. The authors, thereafter, went beyond the technique itself to attempt to explain the effects of the synthesis temperature on the resulting gel morphology. They concluded that the heterogeneous gel possessed a bicontinous domain structure consisting of domains dense and sparse in polymer chains. As we shall see in Section 3.1, this model concurs well with our observations.

The third method is one more suitable for thin polymer films than bulk gels – atomic force microscopy (AFM) [67]. Using this method, a thermosensitive hydrogel was probed in the swollen state under water using the tapping mode. A hot stage was used to regulate the temperature and observe the changes in the gel morphology at higher temperatures. A change in the domain structure was observed on heating. This corresponded to the coil-to-globule transition associated with the LCST. The same technique was not used to image porous hydrogels.

Many other authors used scanning electron microscopy (SEM) to obtain images of porous gels. Gotoh *et al.* used SEM to study the gel microstructure [64]. A porous structure was observed in the case of PDEA synthesized above the LCST and in the case of PNIPAM gels synthesised at any temperature, even below the LCST. Kabra *et al.* [62] also observed their hydrogels by SEM following freeze-drying, as did most of the authors working on polymeric biomaterials.

Miura *et al.,* on the other hand, chose to image their gels using phase-contrast optical microscopy [63]. Two-dimensional Fourier transformation of the real space image produced wave space information, equivalent to the results obtained by light scattering. Light scattering was taken to be a measure of the sample inhomogeneity.

Wu *et al.* used solute exclusion techniques to determine the porosity of the hydrogel [60]. In this method, flourinated probes were driven into the gel and through fluorescence spectrophotometry, the volume fraction of pores larger than the probe size was calculated. Permeation kinetics was also studied. As expected, the phase-separated hydrogels contained larger pores than the conventional gels. Kabra *et al.*

measured the effective porosity by measuring the amount of solvent expelled under mechanical pressure [62].

Apart from data concerning morphology, the other properties of porous hydrogels have hardly been investigated and the limited results are contradictory. Through temperature cycling of the sample, Gehrke *et al.* [59] were able to show that the shrinking kinetics of the porous gels were far superior to those of conventional gels – an observation that was further corroborated by researchers in Hoffman's group [61]. However, the time taken for a dry gel to reach equilibrium swelling did not differ substantially for the conventional and porous hydrogels. Hoffman *et al.* also showed that the swelling ratios of phase-separated gels were higher than those of conventional gels while Gotoh *et al.* claimed the opposite. These contradictions will be elaborated upon in Section 3.2.

A highly original method used to study the swelling and dehydration behaviour of thermoresponsive hydrogels, was put forward by Kato and Takahasi [68]. Using NaCl and KCl as probes, the deswelling mechanism of conventional and macroporous thermoresponsive hydrogels was studied. These metal chlorides were used to study the interaction between the water molecules and the polymer chains, as addition of metal salts into the gel decreased the hydration of the polymer chains, thus affecting its swelling and deswelling kinetics. It was shown that the apparent activation energy for the deswelling of the conventional gel in water was larger than that of the macroporous gel in water. The split process of the skin layer, which was formed on the surface of the gel by heating from outside the gel, was considered the rate-determining step in the case of the conventional gel. The deswelling rate of the macroporous gel was about 100 times faster than that of the conventional gel. This was attributed to the fact that the pore size on the surface of the macroporous was larger than that on the conventional gel.

1.7 Microsyneresis in Polymer Systems

Any study of porous thermoresponsive hydrogels would require an understanding of the underlying process that creates a porous structure – *microphase separation* (MPS) or *microsyneresis*. Microsyneresis in polymer gels, is the process

brought about by simultaneous crosslinking and phase separation. In the case of thermoresponsive hydrogels, heating the pre-gel solution above its LCST drives the system towards phase separation while crosslinking prevents it from total separation into two phases. In other words, this process can be likened to a phase demixing process arrested or "pinned down" by crosslinking. In a microphase-separated structure, discrete hydrophobic microdomains alternate with water-filled voids or pores. Microphase separation, as a general phenomenon, is prevalent in a variety of systems including metal alloys, polymer blends, polysoaps, emulsions, interpenetrating networks, polyelectrolyte gels and biopolymers. It is interesting to note that most biopolymer gels have a microphase-separated structure and hence are usually opaque in appearance [70]. A classic example is cooked egg white.

In general, microphase separation occurs through *spinodal decomposition.* Spinodal decomposition is a phase separation process which results in an *interconnected* or *percolated mesoscopic structure*. Petschek and Metiu defined the spinodal decomposition process as one in which a two-component mixture in a thermodynamically unstable region separates into two equilibrium phases [71]. This is represented in Figures 3.1 and 3.2. Microphase separation in Figure 3.2, can be thought of as an intermittent state between a single phase system and two macrophases.

The phenomenon of microphase separation has been intensively studied by theoretical polymer physicists. Khokhlov, one of the foremost authorities on microphase-separated polymer systems, often uses the term supercrystallization to describe microsyneresis [72]. Such a term reflects the fact that microsyneresis leads to the growth of ordered domains at a mesoscopic level.

It is evident from this literature survey that while substantial work has been carried out in the field of thermoresponsive porous hydrogels, we are a long way off from fully understanding the phenomenon of microphase separation in thermosensitive hydrogels and how it affects their properties. A lot of questions remain unanswered. It is unclear how a phase-separated microstructure affects the swelling ratio – one of the key characteristics of hydrogels. Moreover, the critical

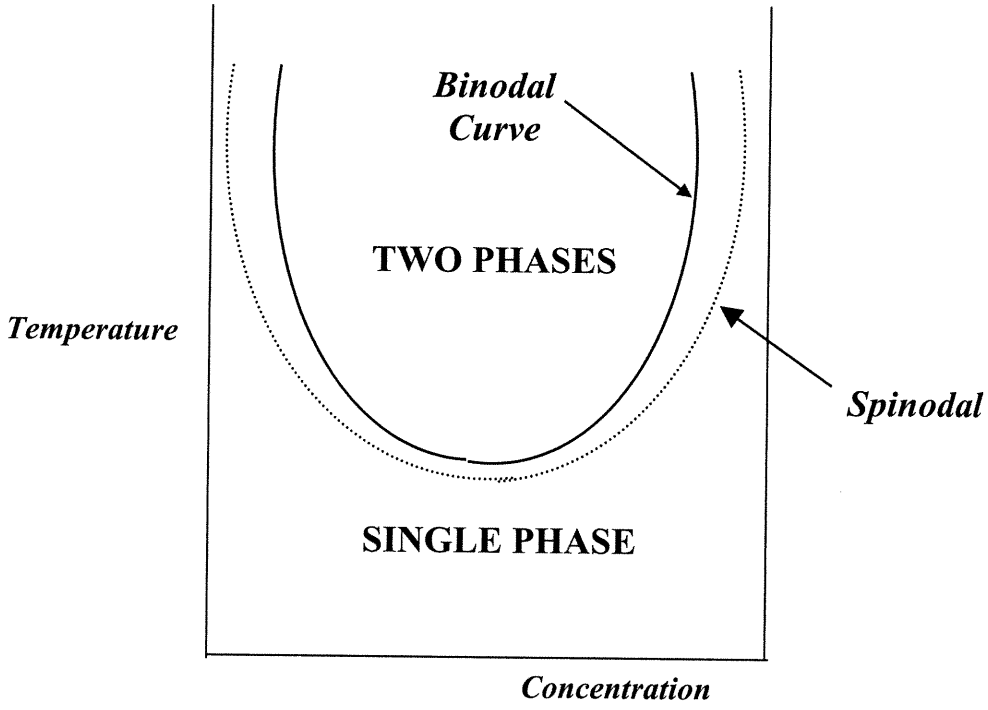

Figure 1.5 General phase diagram depicting area of phase separation. The area above the binodal curve corresponds to total phase separation whereas the area between the spinodal curve and the binodal curve, corresponds to the region of microphase separation. The points on the binodal curve correspond to the LCST for a given concentration.

(a) (b)

Figure 1.6 Conceptual sketch of (a) total phase separation and (b) microphase separation for a mixture of two components, in this case, polymer network and water. (b) is often the result of spinal decomposition. The dark region corresponds to the polymer phase and the white region corresponds to the water phase.

behaviour of thermoresponsive porous hydrogels has not been examined. No further studies have been done to ascertain whether other synthesis variables such as crosslinker concentration, accelerator concentration or mould geometry could also cause microphase separation or microsyneresis in thermoresponsive hydrogels. Furthermore, we noticed little work carried out on porous hydrogels based on PDEA.

On a more fundamental level, the exact mechanism of microphase separation or microsyneresis remained unclear, as did the mechanism of swelling and phase separation for heterogeneous gels. It is clear that a range of factors such as the size of the aggregates, their density and their distance from each other, all could influence the swelling and dehydration profile in porous hydrogels. Also while the kinetics for swelling and shrinking improves dramatically in the case of phase-separated hydrogels, it was clear that the time taken for a dry gel to reach equilibrium swelling does not improve substantially. This could be attributed to the effect of drying methods on the gel morphology, yet another crucial synthesis variable that had been overlooked.

Another aspect which needed to be worked on are the methods used to observe the porous structures in hydrogels. Scanning electron micrography (SEM) was generally the method of choice in the studies cited above. However, it is highly probable that the images obtained by SEM might not accurately reflect the actual morphology of the sample. This is because most of the gels are freeze-dried prior to analysis – a method, as we have seen above, is in itself one used to create pores. Thus, the morphology could have been altered during the drying process. Moreover, not a single article amongst the ones cited above, have shown images of non-porous hydrogels alongside their porous counterparts that could have afforded a comparison of the two.

Finally, the focus of the studies mentioned so far was to improve the swelling and dehydration kinetics of the hydrogels. Other properties and potential applications of such hydrogels had not been explored. Such hydrogels that are thermosensitive and porous, with discrete hydrophobic and hydrophilic domains could be exploited for a wide range of applications.

1.7 Research Objectives

Based on the above literature review and the ensuing discussion, the following plan of study was set forth:

a) **Preparation of thermoresponsive porous hydrogels:** Our starting point in this study was the synthesis of microporous thermoresponsive hydrogels based on *N,N*-diethylacrylamide through temperature-induced and crosslinking-induced microphase separation followed by the study of the influence of other synthesis variables such as accelerator concentration, drying methods and mold geometry on the gel morphology (Sections 3.1, 3.3 and 3.4). To enhance the versatility of these materials, a hydrogel with a pore gradient has been synthesized (Section 3.5.1).

b) **Theory and characterization:** In order to compare the physicochemical properties of conventional and porous thermoresponsive hydrogels, the turbidity and water absorption capacity of these gels was measured. Thereafter, images obtained through optical microscopy afforded a comparison of their morphology. This data was then synthesized into a qualitative model to correlate synthesis conditions with microstructure and swelling behavior (Section 3.1). Once the relationship between synthesis conditions and swelling behaviour was established, we proceeded to compare the phase-transition behavior of conventional gels and porous gels. Two techniques – gravimetry and turbidimetry, were used. The results obtained were used to construct a simple model to explain the LCST phenomenon in conventional gels versus phase-separated gels. A study of the dehydration/ recovery profile of conventional and porous hydrogels was also carried out (Section 3.2.2).

c) **Applications:** In Section 3.5, we demonstrate the use of thermoresponsive hydrogel with a pore gradient, as shape-memory materials and gel actuators. This is followed by a brief discussion of the possible industrial and biomedical applications of these gels.

2. Experimental Section

2.1 Synthesis of Thermoresponsive Porous Hydrogels

All the gels were synthesized in a glass vial of diameter 4 cm. The monomer *N,N*-diethylacrylamide (DEA) was synthesized, distilled and characterized according to a method already described [69]. The crosslinking monomer methylene bisacrylamide (MBA) was purchased from Aldrich and used as received. Ammonium persulphate, the initiator, was purchased from Aldrich and recrystallized in methanol.

The control sample was prepared as follows: 0.2 g of DEA (1.6 mmol) and 0.006 g of MBA (0.04 mmol) were dissolved in 2 ml of distilled water. 0.002 g of ammonium persulphate (0.009 mmol) was added to this mixture. The vial was sealed, nitrogen gas was allowed to bubble through the mixture for about 10 minutes. This is a very critical step, for it ensures total gelation of the solution without any supernatant liquid on the top. It also ensures reproducible gel points for samples of the same composition. The reaction mixture was allowed to react at room temperature. The solution gelated at around 10-15 minutes. The gel was left overnight for the crosslinking reaction to proceed towards completion.

Thereafter, the gel was removed from the mould and soaked alternatively in cold (at room temperature, below the LCST) and hot water (at 40°C, above the LCST) to leach out the sol fraction (residual monomer, initiator, crosslinker). This process was repeated many times, till the wash liquid remained clear on being heated. The gels were then left to soak in cold water for 48 hours. They were then oven-dried to determine the yield, only after all the tests were carried out. This was done to avoid the changes in morphology that can occur during the drying process. The yield obtained was more than 95% in all cases. The gel composition indicated above was used as a standard composition for all porous hydrogels prepared using the TIPS method.

2.1.1 Temperature-Induced Phase Separation (TIPS) Process

To study the effect of time before and during phase separation on the gel microstructure, four different TIPS schemes were devised.

- **Process A:** Gelation carried out entirely above the LCST at 40°C overnight.
- **Process B:** Gelation initiated above the LCST, then allowed to react at room temperature.
- **Process C:** Gelation initiated at room temperature, then allowed to react at 40°C.
- **Process D:** Gelation initiated at room temperature, allowed to react at 40°C for a certain time interval, then made to react at room temperature.

The above processes are depicted in Figure 2.1. To carry out TIPS, an oil bath was maintained at 40°C. At the designated time intervals (Table 3.1), the vials were immersed and subsequently removed from the oil bath. The gels were washed using the same method described in the previous section.

2.1.2 Crosslinking-Induced Phase Separation (CLIPS) Process

In this case, we prepared two samples, a lightly-crosslinked gel with a crosslinker concentration of 0.002 g (0.013 mmol) in 2 ml of water and a higher-crosslinked gel with 0.01 g (0.06 mmol) of MBA in the same amount of solvent. The monomer and initiator concentrations were the same as that for the control sample. As with the case of the control sample, the monomer and crosslinker were dissolved in water. The initiator was then added. The solution was then degassed under nitrogen, sealed and allowed to gel.

Monitoring of CLIPS through Spectrophotometry: The pre-gel solution used to prepare the control sample (see section 2.1) was poured into a UV cell. The mixture was quickly sealed. In this case, we did not degas the mixture so as to prolong the gelation time. The cell was placed in a Cary UV-vis spectrophotometer and the light transmittance of the solution was monitored as a function of time. The same experiment was repeated for the sample with 0.06 mmol of MBA. A water bath connected to the instrument was maintained at 25°C.

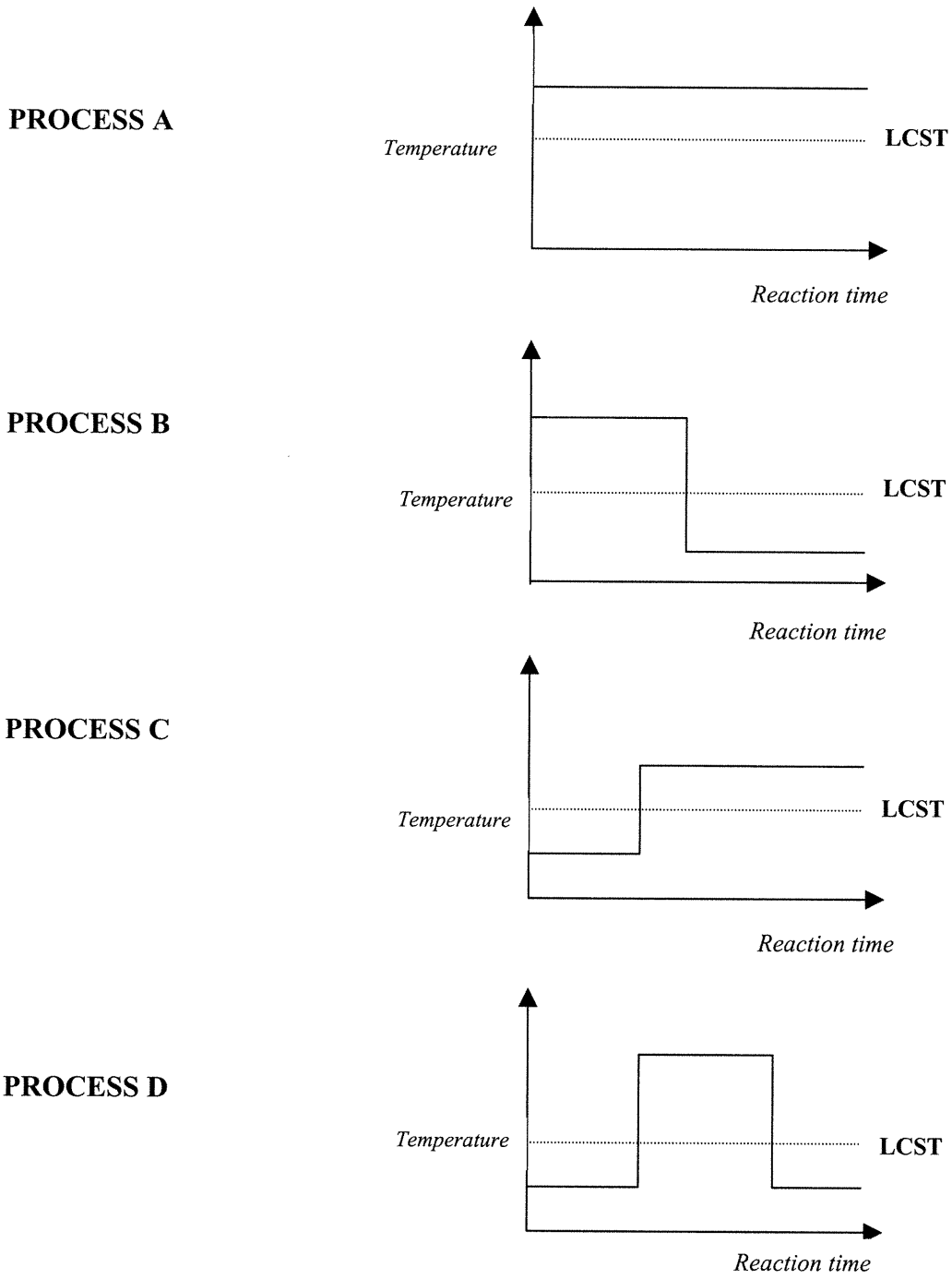

Figure 2.1 Illustration of the phase-separation schemes used to create thermoresponsive, porous hydrogels. Process A refers to the gelation reaction entirely above the LCST. In Process B, the reaction was initiated above the LCST allowed to continue below the LCST. Process C involves initiating the reaction at room temperature and thereafter heating the reaction mixture above LCST. Process D involves initiating the reaction below the LCST, heating the reaction mixture to above the LCST and then allowing the reaction to proceed towards completion below LCST.

2.1.3 Drying of Hydrogels

In order to determine the effect of drying methods on the gel morphology and swelling kinetics, we cut the control gel sample into three pieces of equal size and submitted each piece to a different drying method. The first piece was dried in an oven at 70°C and the second piece was allowed to soak in acetone for 24 hours to permit solvent exchange before it was dried in the oven. The third sample was immersed in liquid nitrogen and, thereafter, freeze-dried until a light, white, Styrofoam-like substance was formed.

To determine their swelling kinetics profile, the dried gels were immersed in distilled water. After every 5 minutes, the gels were removed and the surface moisture was blotted out with a piece of tissue paper. The weights of the gels were recorded. This swelling profile was monitored for one hour.

2.2 Characterization of Conventional and Thermoresponsive Porous Hydrogels

2.2.1 Water Uptake Measurements

To determine the amount of water absorbed at equilibrium, the gels were immersed in distilled water at room temperature for 24 hours. The gels were then removed from the water, blotted lightly with a filter paper and weighed. The swelling ratio (SR) was determined according to the following equation :

$$SR = (W_s - W_d) / W_d$$

where W_s and W_d are the swollen and dry weights of the gel respectively.

2.2.2 Determination of Opacity and Cloud Point

To determine the opacity of each gel, the gel disks were cut into rectangular strips and carefully placed against the wall of an UV cuvette filled with distilled water. Light transmittance was recorded at 600 nm on a Cary UV-vis spectrophotometer. To determine the cloud point, the gels to be analyzed were cut

into thin rectangular strips approximately 0.5 mm thick. This was done to ensure quick heat transfer. These strips were made to lean against the wall of a UV cuvette filled with distilled water. The heating rate was fixed at 1°C/min. Light transmittance was recorded at temperatures from 25 to 50°C, with readings taken every 1°C.

2.2.3 LCST Determination through Gravimetry

To determine the weight change on heating, an oil bath attached to a thermostat was used. The gels, immersed in water, were allowed to equilibrate at each temperature for 30 minutes. Thereafter, the gel was removed from the oil bath, quickly blotted with a filter paper and weighed. This process was repeated for temperatures from 25 to 50°C with readings taken every 1°C .

2.2.4 Deswelling-Recovery Kinetics Profile

To determine the rate of dehydration, the oil bath was set at 50°C. The gels were immersed in distilled water, maintained at 50°C. The gels were removed every 5 minutes, their surface bloated with filter paper and then weighed. This procedure was continued until the gel attained constant weight. To determine the rate of recovery, the shrunk samples were immersed in water maintained at room temperature, and the weight was recorded every 5 minutes for one hour.

2.2.5 Examination of Gel Microstructure

To determine the microstructure of the gel, we selected a technique that was simple, non-invasive and allowed for imaging in the swollen state. To image the samples through inverted optical microscopy, the gels were cut into thin slices. The instrument used was a Metallovert® inverted optical microscope generally used for the analysis of polished metal surfaces. The surface to be analysed was placed over a narrow slit, under which light from the objective was shone. The samples were imaged using the dark-field/light-field mode. The light filters were adjusted to obtain optimal contrast. Images were taken at magnifications of X50 and X100. The images were captured on Snappy® Imaging software. The contrast in the images were

slightly enhanced using the contrast function available in the software. No further digital enhancements were carried out.

2. 3 Applications of Thermoresponsive Porous Hydrogels

2. 3.1 Thermoresponsive Shape-Memory Hydrogels

To create shape-memory materials, the standard gel composition was poured into a test tube. A few drops of *N,N,N,N'*- tetramethyl ethyldiamine (TEMED) were added (10 μl for a 2 ml solution) slowly to prevent the droplets from quickly settling to the bottom. This created a pore-gradient with the top portion opaque and the bottom portion transparent and the middle section slightly cloudy. To create a gel cylinder with both ends opaque (porous), one end of the cylinder into an oil bath kept at 50°C to induce phase separation, while a few drops of TEMED were added to the other end. The tubes were then cracked open, the gels carefully removed and washed using the same method described earlier. The synthesis scheme for the same is described in Figure 2.2.

To demonstrate the shape-memory effect, the shape of the gel was recorded at room temperature. The gel was then immersed in hot water and left for 10 minutes to equilibrate. The change in shape was noted visually. The sample was able to recover its original shape on cooling.

2.2.6 Thermoresponsive Gel Actuators

To demonstrate the potential application of thermoresponsive hydrogels as gel actuators or artificial muscles, we synthesized a thermoresponsive hydrogel with a pore gradient in a glass tube by using the TIPS method. To obtain a gel with both the ends opaque and the middle section transparent, a few drops of TEMED were added to the surface of the gel while the other end of the tube was immersed in an oil bath maintained at 40°C. The gel so obtained was removed from the glass tube and washed. It was then made to suspend in water with its two ends hanging parallel to each other. When the gel was heated to above its LCST, the gel shrank dramatically with the two ends of the gel coming together, thus displaying a finger-like motion.

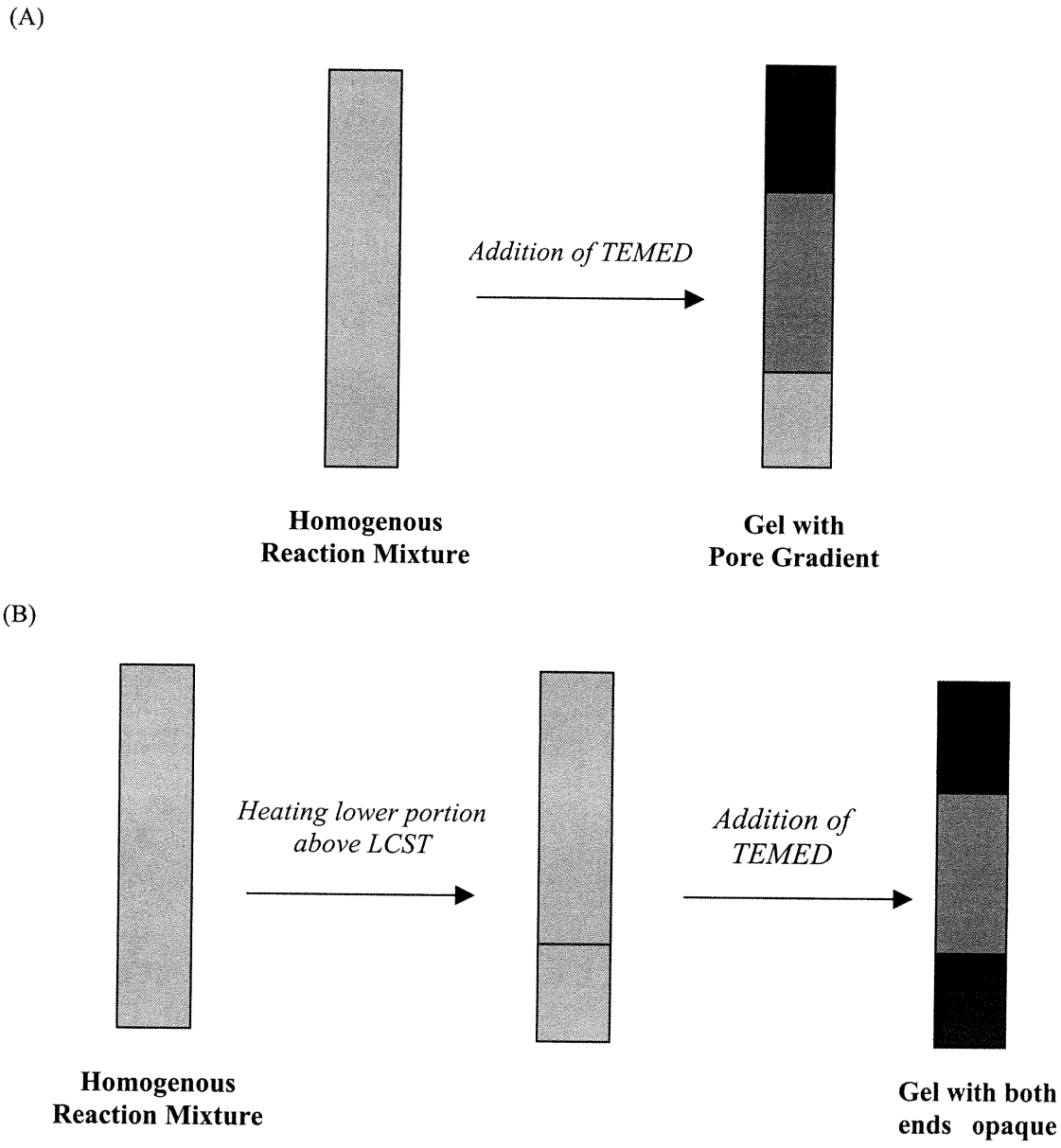

Figure 2.2 Methods used to create thermoresponsive hydrogels with a pore gradient through (a) addition of TEMED and (b) addition of TEMED while heating portion of gel mixture above the LCST. Long glass tubes are used as moulds. In (a), the reaction mixture is transferred to the mould to which a few drops of TEMED (10 µl for a 2 ml solution) are added. As the rate of reaction is faster than the diffusion of TEMED throughout the gel mixture, the top portion of the gel is able to consume more TEMED and hence turn opaque, while the lower portions are less opaque, with the opacity decreasing as a function of the depth of the surface. In (b), TEMED is allowed to permeate from the top while the bottom portion of the tube is immersed in an oil bath kept at 40°C. This portion undergoes microphase separation during gelation thus forming an opaque porous region.

3. Results and Discussion

3.1 Mechanism of Microsyneresis in Thermoresponsive Hydrogels

To our knowledge, no detailed theoretical study of the microphase separation process in thermoresponsive hydrogels has been undertaken. While complex phase diagrams and mathematical calculations are beyond the scope of this thesis, what will be presented here is a phenomenological overview of the process based on the observations and data obtained. Conceptual sketches are used to illustrate the phenomenon and give the most probable explanation of the process as it occurs at the molecular level and thus, predict the resulting conformational changes at the mesoscopic level. Classical theories in colloidal science, especially those dealing with microemulsions have been applied. It is hoped that this model will serve as a framework to build more complex quantitative models of microphase separation in thermoresponsive hydrogels.

Though the underlying phenomenon of both are the same, we have chosen to consider temperature-induced MPS and crosslinking-induced MPS have been considered as two different processes, and, therefore, they will be treated separately.

Strictly speaking, all hydrogels, even the transparent ones, are all porous, as voids exist throughout the network. However, these conventional gels contain pores on a sub-micron scale - pores that are too tiny to allow for solvent uptake through capillary action. The hydrogels synthesized in this study would be considered microporous gels, since they contain domain structures in the range of micrometers.

The starting point in this case, is the basic model established by S. Gehrke and A. Hoffman [59, 61]. In his earlier work on this subject, Gehrke hypothesized a simultaneous phase separation and crosslinking process that would result in the creation of voids or pores. In other words, it is a phase-separation process frozen in by the presence of crosslinks. The assumption was that this phase separation would occur through spinodal decomposition and produce a classic bicontinous structure.

One would get a clearer picture by referring back to the phase diagram (Figure1.6). According to this diagram, microphase separation occurs at a certain critical temperature interval hovering around the LCST. The system is in a metastable

state and any further increase in temperature would lead to total phase separation. Therefore, the aim here is to "lock in" this metastable state through crosslinking. This would produce a microphase-separated structure where polymer microaggregates alternate with voids or pores.

Allan Hoffman developed on the idea put forward by Gehrke by proposing a conceptual sketch of this phase-separation-induced pore-formation process as illustrated in Figure 3.1.

(a) (b)

Figure 3.1 Model of (a) Conventional gel and (b) porous phase-separated gel as visualized by Hoffman *et al.* [61]. The dark globules in (b) represent hydrophobic microaggregates and the voids so formed represent micropores.

According to this figure, heating the thermoresponsive hydrogel above the LCST causes the hydrophobic side chains to aggregate thus creating larger voids in the network. We have chosen the above model as a reference point to qualitatively describe microsyneresis in thermoresponsive hydrogels. On a mesoscopic level, the key feature of porous or phase-separated hydrogels are their hydrophobic aggregates. Here, three factors come into play – the number of hydrophobic aggregates, the size of the aggregates and the distance of the aggregates from each other. If we were to liken the aggregates in a hydrogel to a microemulsion, then three mesoscopic structures are possible. These models are illustrated in Figure 3.2.

In the first case (Model A), the aggregates present are very small and the distance between them very large. The aggregates are held together by flexible linear polymer chains and crosslinks.

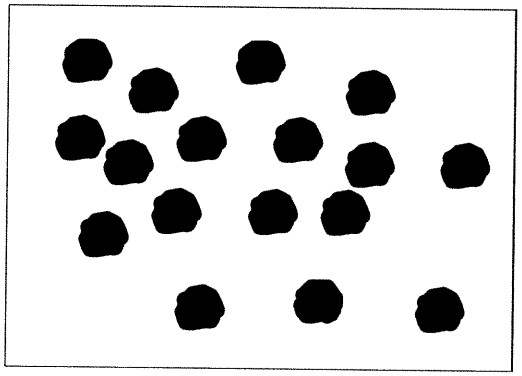

MODEL A

Continuous Phase: Water

Dispersed Phase: Hydrophobic aggregates held together by crosslinking molecules

Properties: Highly fragile gel with high swelling ratio

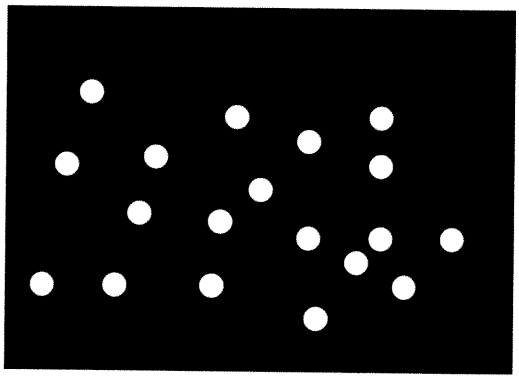

MODEL B

Continuous Phase: Polymer Marix

Dispersed Phase: Water

Properties: Firm, low swelling ratio

Porosity: Closed pores

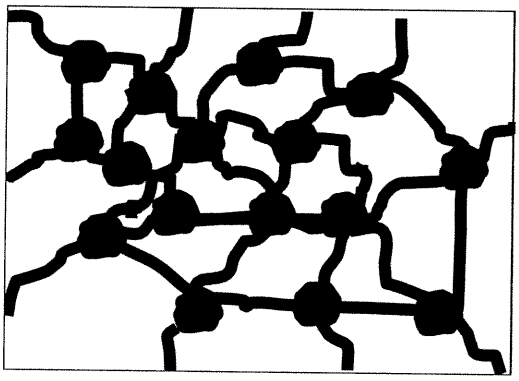

MODEL C

Bicontinuous water and polymer phases

Properties: Firm, high-swelling ratios

Porosity: Interconnected Pores

Figure 3.2 Models of possible mesoscopic structures in phase-separated hydrogels.

It is apparent that in such an arrangement, where the water is the continuous phase and the aggregates, the dispersed phase, would produce highly fragile structures that are closer to a latex, rather than a gel. The swelling capacity of such a structure would be high while the mechanical properties would be extremely weak. The reverse is true for Model B, where we see water islets trapped in a hydrophobic matrix. Here the swelling capacity would be very low while the mechanical properties would be good. The third case (Model C) is a bicontinuous structure where both the solvent phase and the aggregates are interconnected. The latter is an ideal case of spinodal decomposition.

The presence of crosslinks keeps the aggregates suspended in the gel matrix "solution". In other words, it plays the role of a surfactant. In a way, just as the hydrophilic-lipophilic balance of the surfactant determines whether the resulting emulsion would be an oil/water or a water/oil mixture, the crosslinker concentration in a hydrogel is a key factor that determines whether the resulting morphology fits into Model A, B or C. It must be noted that none of the gels synthesized here would perfectly fit in within any of these three theoretical models. We would only be able to approximate the experimental data to these theoretical models.

The swelling and turbidity data for all these gels are given in Table 3.1. Through extrapolation, the data obtained has been used to interpret the mechanism of simultaneous phase separation and crosslinking in thermoresponsive hydrogels. Optical microimages of the gels so obtained are given in Figure 3.5.

3.1.1 Temperature-Induced Phase Separation

In this series, the synthesis was carried out under two sets of conditions – in the first case, we initiated the polymerization below the LCST and in the second case, above the LCST. The LCST of PDEA is around 32°C, hence 40°C was considered a suitable temperature above the LCST. Within each series, we varied the reaction time above the LCST and the reaction time below the LCST.

Reaction initiated above the LCST: In this series, the pre-gel solution was immersed in an oil-bath immediately after sealing and degassing the mixture. In Process A, the pre-gel solution was left at 40°C overnight, while in Process B, the reaction mixture

was removed at two different time intervals and the reaction proceeded to completion at room temperature. The following observations were recorded:

Within the first few minutes of placing the reaction mixture in the oil bath, the solution turned cloudy. This corresponds to the aggregation of linear polymers and micro-networks in the solution. In the first case, when we left the solution overnight at 40°C, we obtained a light, fluffy, gel-like structure that was highly fragile and was unable to retain it disk shape once removed from water. This suggests that a very sparse network, i.e. of low density, had been formed. The gel was opaque, which suggested that hydrophobic microdomains were present. The high swelling ratio and extremely poor mechanical properties suggested that it contained large water-filled voids or pores. Being highly fragile, the gel could not be used to obtain optical microscope images or for any further analysis.

It was apparent that keeping the gel for too long above LCST rendered the gel fragile. Therefore, the gel was removed from the oil bath at various time intervals. We found that even half an hour above the LCST produced a highly swollen and fragile gel. The only durable gel obtained was after ten minutes of gelation above the LCST. The water uptake for this gel was far lower than that of the gel synthesized totally above the LCST, but twice as much as that of the control sample (Table 3.1).

Based on the above observations, we have proposed the following model to describe temperature-induced phase separation for gelation reactions initiated above the LCST. Figure 3.3 presents a pictorial representation of the mechanism described below.

When the reaction proceeds above the LCST, the first linear polymeric chains are formed. These chains can either (a) react with other monomer units to form longer polymeric chains or (b) react with a crosslinker unit to form a micronetwork. Only those chains that are long enough will aggregate. We assume that the chain has to be of a certain critical length or molar mass to aggregate. (Results published so far in the literature make no mention of such a parameter, but indirect evidence suggests that the thermosensitive chain has to be of a certain length to undergo aggregation. Size exclusion chromatography coupled with light scattering techniques might be used to establish the same).

Table 3.1 Water Absorption and Turbidity Data

Phase-Separation Method	Process Description	Appearance & Texture	Light Transmittance at 600 nm	Water Uptake (wt/ wt)
TIPS Process A	Totally above LCST	Opaque, sponge-like texture; highly fragile	No data *	~ 55 *
TIPS Process B	Removed after 15 min	Fragile opaque gel	0.7	40.8
	Removed after 10 min	Firm opaque gel	0.6	21.9
TIPS Process C	15 min/R.T. ; overnight/40°C	Non-uniform gel with clear and opaque layers	No data **	No data **
TIPS Process D	5 min/R.T. ; 10 min/LCST	Fragile opaque gel	0.8	18.62
	10 min/R.T. ; 10 min/40°C	Firm opaque gel	1	18.06
	10 min/R.T. ; 5 min/40°C	Non-uniform with clear core and opaque rim	No data **	No data **
CLIPS	Control Sample	Firm, slightly cloudy gel	64.3	10.15
	Reduced crosslinking	Transparent, slightly fragile gel	96.6	17.75
	Increased crosslinking	Firm opaque gel	1.2	7.8

* Sample too fragile to allow for accurate measurements

** Cannot be determined due to macroscopic heterogeneities

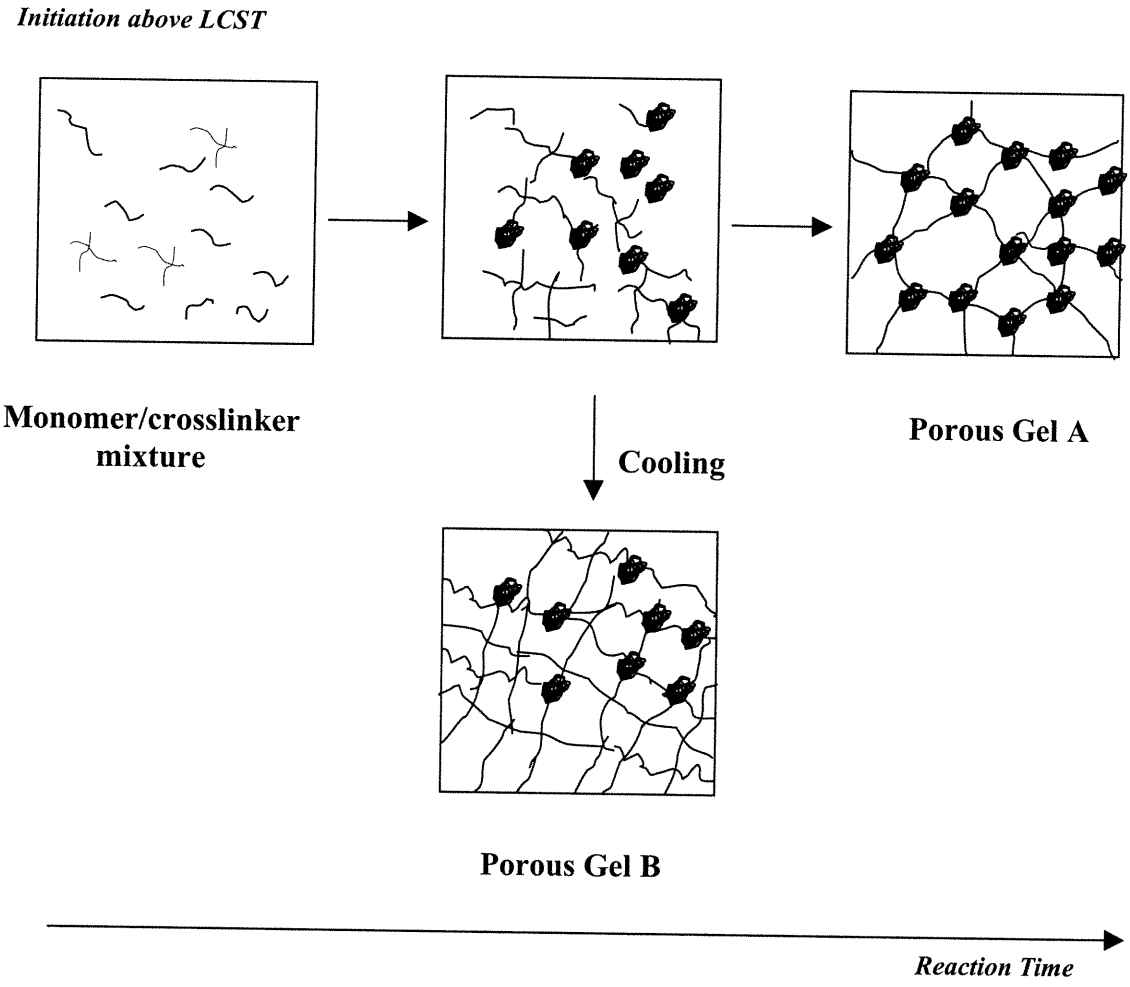

Figure 3.3 General scheme of the gelation reaction, initiated above the LCST. Single curves represent linear polymers, the crosses represent the crosslinker molecules and the dark globules represent the hydrophobic microaggregates. Porous gel A represents a highly porous network solely composed of aggregates while porous gel B represents a partially porous gel where some of the aggregates have been allowed to uncoil and recover their original conformation on cooling.

The other short polymeric chains that cannot undergo aggregation would simply hold the aggregates together. Also the ongoing crosslinking reactions plays the role of preventing phase demixing and by keeping the aggregates in a 'frame' or network. The aggregates are rather small. Ordinarily, such aggregates should precipitate and settle at the bottom of the glass vial thus rendering the gel macroscopically inhomogenous. We assume that the heat here causes the particles to be in constant thermal motion thus preventing precipitation.

Now, if the crosslinking process is allowed to continue above the LCST, we obtain a sparse phase-separated network consisting of small aggregates held by crosslinks and linear polymer chains (Figure 3.3 – Porous gel A). The resulting pores or water-filled voids are large. Experimental data and visual inspection support our model – the resulting gel is highly fragile and opaque rendering it too fragile for further analysis. We have roughly estimated the swelling ratio of the hydrogel to be about 55 – five times that of the control sample. The mesoscopic structure of such a gel is close to that of Model A (Figure 3.2), i.e., small hydrophobic aggregates with large-water filled voids.

On the other hand, if the crosslinking process is allowed to continue below the LCST (Process B), a different scenario unfolds: Firstly, those aggregates that have yet to be locked-in through crosslinks have an opportunity to recover their original conformation (Figure 3.3 – Porous gel B). Secondly, it allows for the formation, at least partially, of a conventional dense network without the polymer chains aggregating. This renders the gel more durable but also lowers the swelling capacity (Table 3.1), as the number of aggregates, hence the size of the pores, is reduced. This would explain why the swelling capacity for the Process A gel is above 55 while the swelling capacity of the Process B – 15 minutes is only 40.8. Swelling data also reveals that, under these conditions, the water uptake is still higher than that of the control sample. The gel synthesized through initiating the gelation reaction above the LCST and removing after 10 minutes has twice the swelling capacity of the control sample. Obviously, the presence of larger pores accounts for the differences in the water uptake capacity of the two. A possible explanation for the significant difference in swelling capacities of the gel left for 10 minutes (swelling ratio of 21.9) and that

left for 15 minutes (swelling ratio of 40.8) could be that there exists a critical point, corresponding to the gel point, between 10 and 15 minutes. Experiments carried out in our laboratory have shown that a sample of the same composition takes about 10-15 minutes to reach its gel point when polymerized below the LCST. It is highly probable that the reaction mixture crossed this threshold when kept above the LCST for more than 10 minutes, since heat accelerates the gelation reaction. Thus, the gel kept for 15 minutes contained permanently locked-in aggregates that could not recover their original conformation on cooling. Moreover, there would have been much fewer crosslinking monomers to create a denser network below the LCST – which explains its fragility. We could say that on a mesoscopic level, the supramolecular structure of the 15-minute gel is closer to Model A (Figure 3.2) – a structure whereby the hydrophobic aggregates are suspended in water through crosslinks, the water being the continuous phase. The 10-minute sample, on the other hand, is closer to that of Model C – a bicontinuous structure that allows for the free flow of solvent yet possesses relatively good mechanical properties due to interconnected aggregates.

Reaction initiated below the LCST: The mechanism for gelation initiated below the LCST is quite different and hence the properties of the gels obtained differ from those examined so far. Figure 3.4 presents a conceptual sketch for the mechanism described below.

In the first case (Process C, Table 3.1), the pre-gel solution was allowed to react at room temperature for 15 minutes and, thereafter, entirely above the LCST. 15 minutes was enough for the reaction mixture to gel. Raising the reaction temperature above its LCST would have caused both macrosyneresis and microsyneresis to occur. In other words, the so-called first spanning network produced at the gel point, would shrink as a whole network above the LCST, thus producing a supernatant solution consisting of unreacted monomers and initiator. These remaining monomers would then form a less dense network above the main network. Thus, a macroscopically inhomogenous gel with two layers is formed. The heterogenous nature of the gel makes it unfit for further characterization.

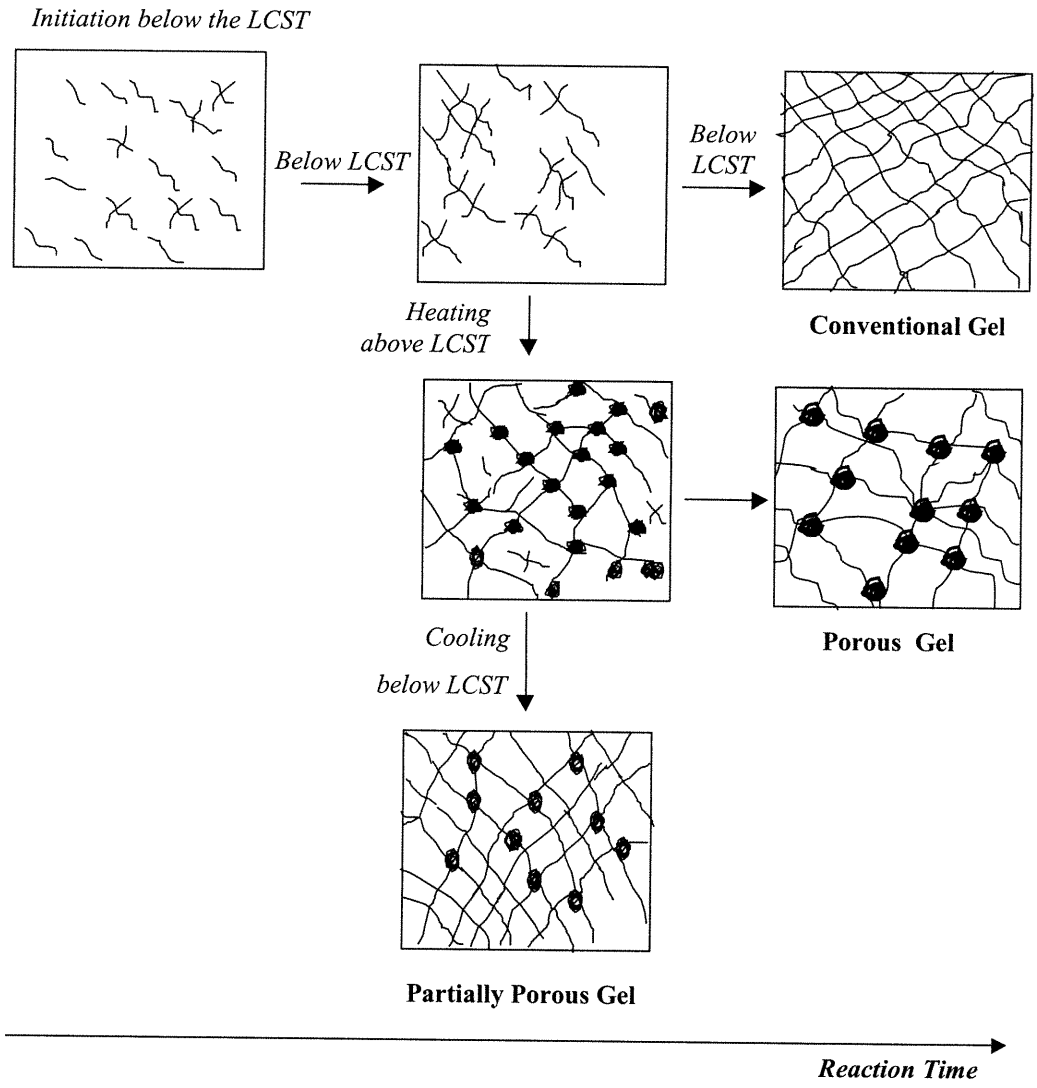

Figure 3.4 General mechanism of a PDEA gelation reaction, initiated below the LCST. Single curves represent linear polymers, the crosses represent the crosslinker molecules and the dark globules represent the hydrophobic microaggregates. Gelation carried out entirely below the LCST produces a conventional non-porous gel whereas heating the reaction mixture after a certain time interval above the LCST causes microaggregation and hence the appearance of pores. Maintaining the reaction temperature above the LCST locks in the porous structure while cooling of the gel allows for some of the aggregates to uncoil and recover their original conformation. The latter leads to a partially porous structure.

allows for some of the aggregates to uncoil and recover their original conformation. The latter leads to a partially porous structure

Finally, the last TIPS scheme involves initiation at room temperature, followed by phase-separation above the LCST and reaction termination at room temperature (Process D). In the first case, the gel is left at room temperature for 5 minutes followed by phase-separation above the LCST for 10 minutes. In this case, the swelling ratio is almost the same as that allowed to react for 10 minutes at room temperature. The only significant difference between these two samples lies in their texture. This is not difficult to understand. The pre-gel solution left to react at room temperature for five minutes had not yet gelled when immersed in the oil bath. Gelation occurred above the LCST, which as we have seen above, creates a fragile structure. On the other hand, allowing the pre-gel solution to react for 10 minutes at room temperature causes gelation below the LCST. This gel, when heated above the LCST, creates aggregates which are "pinned down" by the existing network. Thus, the mechanical properties of the gel are improved. It must be noted that 10 minutes above the LCST is short enough to prevent macrophase separation (Process C).

In this same series (Process D), the time above phase separation was shortened. Here the result was quite predictable. Short phase-separation times above the LCST do not allow the heat energy to permeate completely or the chains to uncoil in a uniform manner throughout the reaction mixture once cooled below the LCST. The result is a macroscopically heterogeneous gel with a clear core and an opaque rim. The non-uniformity of the gel makes it unfit for further characterization.

In an article on microphase separation in binary polymer fluids [73], the author was able to deduce, through complex calculations, that at a certain critical composition, a transition occurred from a percolated (interconnected) bicontinuous phase structure to a droplet (close-celled) morphology. Likewise, in the case of thermoresponsive porous hydrogels, this would mean that certain synthesis conditions would create either an open-celled or close-celled porous structure. A similar change in morphology between Processes B and D can be observed (Figure 3.5). This suggests that allowing the gel to react at room temperature below the LCST creates

(a)

(b)

(c)

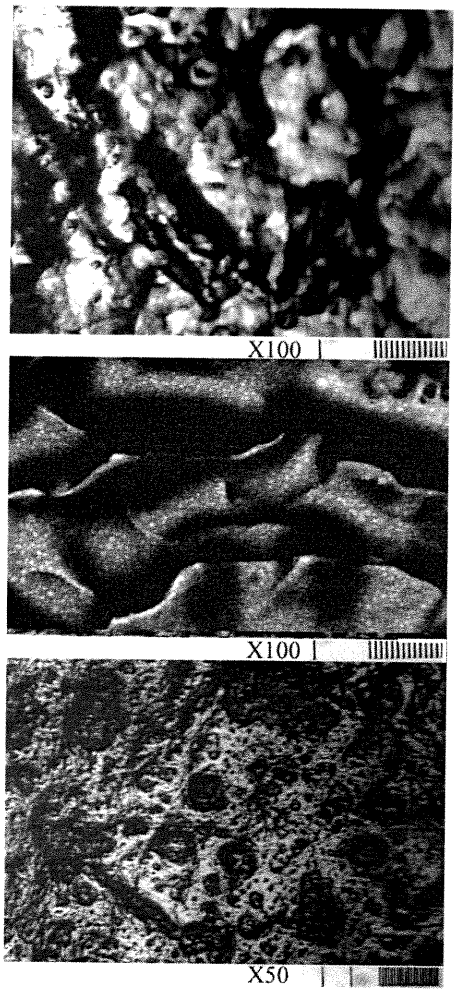

Figure 3.5 Influence of the TIPS process on the gel microstructure. (a) control sample – 0.006 g MBA in 2 ml of water; (b) gel obtained through Process B- gelation initiated above the LCST; (c) gel obtained through Process D – gelation initiated at room temperature. Each division on the scale corresponds to 10 μm

conditions that favor the formation of the close-celled structure over the open-celled structure.

In terms of the mesoscopic models that we have put forward, Process D might lead to a structure resembling Model B (closed pores). This could also explain why the swelling ratio of the gels synthesized through Process D was lower than that synthesized through Process B. The optical images show that the gels created through Process D have a partially closed structure (Figure 3.5). Many of the pores are isolated and are not accessible to the solvent. It is possible that at a certain critical reaction time, there is a morphological transition from an open-cell structure to a close-cell structure. To corroborate these conclusions, more work is needed by further modulating the reaction time before, during and after phase separation. A similar trend was observed in the case of hydrogels synthesized through crosslinking-induced phase separation, as discussed in the next section.

The above discussion provides an overview of the TIPS process and their effect on gel morphology and water uptake properties. Here is a brief summary of our observations.

Summary of observations for reaction initiated above the LCST:

- A gelation reaction initiated and maintained above the LCST produces a highly fragile structure with large pores and hence, a high swelling ratio.
- Once initiated above the LCST, allowing the reaction to continue below the LCST causes some of the hydrophobic aggregates to recover to their original conformation thus creating a partially dense network. This improves the durability of the gel but decreases its water absorption capacity.
- If the pre-gel reaction mixture crosses its gel point while kept above the LCST, the resulting gel will be more fragile and swell more when cooled. Likewise, if a pre-gel solution crosses its gel point only after being cooled, the resulting gel will be firmer and will swell less (Table 3.1 – Process B).
- Generally, macrophase separation (total separation of the liquid from the gel matrix) will not occur for a gelation reaction initiated above the LCST.

Summary of observations for reaction initiated below the LCST:

- If the reaction mixture is allowed to reach its gel point below the LCST, then heating the solution above its LCST will cause macrophase separation as the network shrinks as a whole. The resulting gel will be macroscopically inhomogenous.
- In Process D (initiation below the LCST, reaction above LCST, continued below LCST), the gel which experienced a gel point above the LCST would be more fragile than the gel whose gel point occurred below the LCST.
- Short phase-separation times above the LCST leads to macroscopic heterogeneities. Long phase-separation times above the LCST renders the gel highly fragile. Thus, a certain optimum time interval between these two limitations must be chosen.

Finally, preliminary results point to reaction time above the LCST favoring an open-cell microstructure, and reaction time below the LCST favoring a close-celled microstructure. This study demonstrates that one can obtain hydrogels with the desired swelling ratios, mechanical properties and porosity by simply modulating the time period before, during and after phase separation. This study also highlights the significance of the gel point as a critical parameter in shaping the morphology and properties of thermoresponsive porous hydrogels.

The above model was conceived based on observations like turbidity and texture coupled with data on the swelling ratio and porosity. The model derived from these observations is also based on theories in colloidal science, especially those concerning microemulsions. This combination of visual observations and quantitative data has led to a comprehensive model that further builds upon the results obtained by Kabra *et al* [62]. In their work, a conceptual model describing MPS in thermoresponsive hydrogels was put forward solely on the basis of SEM microimages. Details of this model are presented at the end of the next section.

3.1.2 Crosslinking-induced Phase Separation

Crosslinking-induced phase separation presents a different picture from the one presented above, though they both lead to microsyneresis and, hence, porous hydrogels. Varying the crosslinker concentration has been used to create porous acrylamide gels for electrophoresis and porous styrene-divinylbenzene resins amongst others. Earlier work on microsyneresis conducted by Dusek of the Czech Republic in the sixties involved creating heterogenous methacrylate-based gels by modulating various synthetic parameters, including crosslinker concentration [74-75]. To our knowledge, no results on crosslinking-induced phase separation in thermoresponsive hydrogels have been reported.

As in the case with other polymer systems, increased crosslinking causes the network to phase-separate since the dense, more hydrophobic network is unable to absorb all the water available. Various theories abound, such as the "locking-in" of the critical concentration fluctuations at the gel point by the crosslinking molecules. In a review on the permeability of hydrogels [76], Steven Gehrke cited the hypothesis of a colleague who visualized a process whereby the formation of any crosslink between two linear chains fixes a region of polymer concentration higher than the bulk. This, in turn, enhances the probability of further crosslinking within this region of high polymer concentration, leading to a cross-linked « microgel » within the gel matrix. Nakazawa and Sekimoto proposed a model of phase separation induced through crosslinking within the spinodal region [77]. They have built a model based on the assumption that crosslinking induces phase demixing of the polymer solution. The other possibility is that crosslinking induces an inhomogenization of the gel and freezes in the inhomogeneities. Whichever way it is interpreted, it is clear that increased crosslinking would lead to a heterogenous microstructure, hence the appearance of voids or pores.

The interpretation for the CLIPS process adopted in this study, is fairly straightforward and is related to the polymer-solvent interaction parameter χ. It is a well-established fact that for polymer solutions, this parameter is concentration-sensitive and there exists a critical polymer concentration at which the solvent becomes a non-solvent [72]. By extending that argument to hydrogels, one can

assume that a certain critical crosslinker concentration will create a network that will render the available amount of solvent a non-solvent. Hence, the network would be unable to absorb all the solvent available and hence be inclined to phase-separate from the solution. Again, as in the case of TIPS, the phase-separation process is in competition with the ongoing gelation process. Thus, the trade-off between these two processes results in a microphase-separated structure. The trend in the swelling behavior is equally straightforward (Table 3.1). Increasing crosslinking increases the hydrophobicity of the network and hence causes a decrease in water absorption. The change in microstructure upon varying the crosslinking concentration is far more interesting (Figure 3.6).

In case of the lightly crosslinked hydrogel, barring a few defects, the topography is uniform (Figure 3.6–a). At higher crosslinker concentrations, we observe the appearance of inhomogeneities. We could interpret the voids as being water channels surrounding hydrophobic domains. On further increasing the crosslinker concentration, a different scenario unfolds: One can observe the appearance of pores, some of them interconnected, some of them isolated (Figure 3.6-c). This could well be an example of the phenomenon described by Barry in his article [73] - the transition from a percolated morphology to a droplet morphology. We find that on increasing the crosslinker concentration, the microstructure passes from a relatively uniform topography to a percolated (interconnected) morphology to a semi-droplet (appearance of closed pores). We can assume that increasing the crosslinker concentration even further would lead to a completely close-celled structure or a droplet morphology. More experiments would have to be conducted to corroborate these observations. Such experiments would involve systematically varying the crosslinker concentration to determine the critical concentration at which this morphological transition would occur.

Thus, one can deduce that on increasing the crosslinker concentration, we approach a microstructure close to Model B – water islets or voids trapped in a hydrophobic matrix. As expected, such hydrogels are rigid with a low water absorption capacity. Thus, one can conclude that the presence of pores alone do not amount to improved water absorption capacities. Depending on the methods of pore-

formation and the nature of the pores, porous hydrogels may have lower or higher swelling ratios than their conventional counterparts.

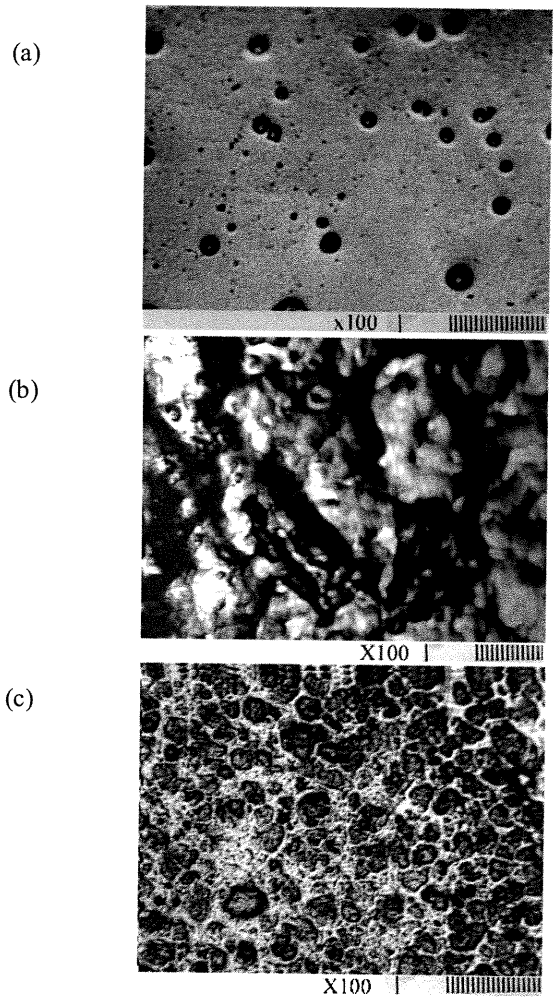

Figure 3.6 Influence of increasing crosslinker concentration on the gel microstructure: Images obtained through inverted optical microscopy. All samples contain 0.2 g PDEA in 2 ml of water.; (a) reduced crosslinker concentration - 0.002 g (0.6 mol%) of MBA in 2 ml of water; (b) control sample – 0.006g MBA (1.9 mol%) in 2 ml of water; (c) increased crosslinker concentration - 0.01 g (3.2 mol %) of MBA in 2 ml of water. Each division on the scale corresponds to 10 μm.

Monitoring of CLIPS through Spectrophotometry: In order to better understand the crosslinking-induced phase separation process, the change in turbidity for both the control sample and the increased crosslinker sample as a function of time, was monitored. For this experiment, we chose not to degas the reaction mixture as that would have led to very short gelation times. The results are shown in Figure 3.7.

It can be seen that while the turbidity of the reaction mixture for the control sample does not change with time, the reaction mixture for the CLIPS sample presents a different picture. After a certain critical time period, one observes a drastic increase in turbidity. This corresponds to the point at which the gel turns opaque.

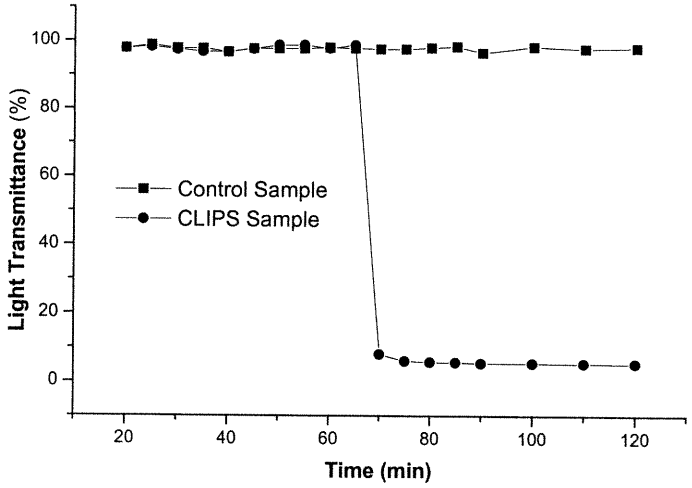

Figure 3.7 Monitoring of gelation reactions for control sample and the CLIPS sample, through light transmittance at 600 nm. The transmittance profile for the highly crosslinked sample displays an abrupt change in transmittance at a certain critical temperature. This critical reaction time is akin to an LCST, whereby the pregel system undergoes phase separation. (Composition:- Control sample: 0.006 g MBA (1.9 mol%) in 2 ml of water; CLIPS sample - 0.01 g (3.2 mol %) of MBA in in 2 ml of water. All samples contain 0.2 g PDEA in 2 ml of water.

It is clear from previous discussions that an opaque appearance suggests phase separation. Thus we can deduce that in CLIPS there exists a critical time, at which point microphase separation occurs. This can be interpreted as follows: As the crosslinking reaction proceeds, the growing network reaches a critical size at which point it is no longer "soluble" in the solvent. At this point, the network tries to separate from the solution but is prevented from completely doing so by the presence of crosslinks. It is also interesting to note the inverted S-curve in the graph, similar to the curve that corresponds to the cloud point or the LCST, as we shall see in Section 3.2.

This gelation kinetics experiment points to the existence of a critical reaction time. This is a critical time parameter akin to an LCST, at which point the pre-gel solution undergoes microphase separation.

It is useful to compare the results obtained so far with those of other researchers working in the field of thermoresponsive porous hydrogels. Kabra *et al.* carried out a systematic study on porous thermoresponsive hydroxypropyl cellulose hydrogels [62]. They concluded that keeping the time before phase separation short and the time during phase separation long enough to lock-in the phase-separated structure, would produce an interconnected porous structure. The SEM images obtained showed a clear transition from a percolated morphology to a droplet morphology on increasing the initial polymer concentration – a parameter that we did not take into account. Similarly, they observed a transition from a closed-cell structure to an open-cell structure, on increasing the time during phase separation, similar to the observations we made. The authors noted that the formation of a permanent interconnected microstructure may be a critical phenomenon, perhaps related to a percolation or gel point – an argument that we have corroborated. Swelling or thermosensitive behaviour of these gels were not studied. It must be noted that hydroxypropyl cellulose gels are far more durable than acrylamide-based gels, hence lend themselves very well to analysis. On the other hand, we were unable to obtain images of our highly swollen, phase-separated structures, due to their fragile, latex-like texture. We would like to emphasize, however, as already pointed out in Chapter 1, that the images obtained through SEM in this study might not fully

correspond to the actual morphology since freeze-drying of gels is itself a method used to induce pores. The effect of drying methods on gel morphology is discussed in Section 3.3.

Other studies on thermoresponsive hydrogels deal less with the theoretical aspects of pore-formation and more on the effect of porosity on the swelling behavior. Wu *et al.* [60] reported that the swelling ratios of macroporous poly(*N*-isopropylacrylamide) hydrogels were significantly larger than that of their conventional counterparts, an observation that we have confirmed. The gels they obtained were synthesized entirely above the LCST. They also noticed the weak mechanical properties of the phase-separated hydrogels as compared to conventional gels. Their phase-separated gels were apparently more durable than ours. This could be due to the fact that they used dihydroxyethylene-bis-acrylamide as a crosslinker rather than methylene-bis-acrylamide. Results obtained for deswelling/swelling kinetics will be discussed in the next section.

On the other hand, the results reported by Gotoh *et al.* contradict our results as well as what has been reported in the literature [64]. They claim that the PNIPAM gels remain opaque even when synthesized below the LCST. In other words, they have concluded that phase-separated structures are formed even below the LCST. One probable explanation could be that they used a critical amount of the crosslinker concentration that could have caused phase separation even at low temperatures. Another reason could have been an excess of TEMED which is the accelerator. As we shall see in Section 3.7, addition of larger amounts of TEMED could also induce phase separation. They also noticed that the swelling ratio of the hydrogels decrease with an increase in synthesis temperature. Since we have not conducted similar studies by varying the temperature, we cannot confirm or refute these claims. It could well be possible that an increase in temperature accelerates the growth of hydrophobic domains thus leading to larger hydrophobic domains and, hence, lower swelling ratios. This study, however, proves that gels synthesized at 40°C generally have a far larger water absorption capacity than their homogeneous counterparts.

Having established the microstructure and water absorption capacities of these thermoresponsive hydrogels, we are now in a better position to interpret their phase transition behavior.

3.2 Thermoresponsive Properties of Phase-Separated Hydrogels

A study of the phase transition behavior of the hydrogels brings out the stark differences between conventional hydrogels and phase-separated hydrogels. The original assumption that porous hydrogels, being already phase-separated, would not undergo any further phase transition at the LCST. This was proven to be wrong. Porous phase-separated hydrogels display a peculiar phase transition behaviour at the LCST. It is a behaviour that differs markedly from that of conventional non-porous thermoresponsive hydrogels.

3.2.1 Phase-transition Profile at the LCST

The phase transition profile of the hydrogels were obtained using two simple methods, the cloud point measurement and gravimetry to compare the phase-transition profile of conventional versus phase-separated thermoresponsive hydrogels. We chose the hydrogel crosslinked with 0.1 g of MBA, as a sample specimen for crosslinking-induced phase separation and the gel removed after 10 minutes of phase separation (Process B) as a sample for temperature-induced phase separation.

As we see in Figure 3.8, the cloud point method and the gravimetric method produce strikingly different profiles, even though they should supposedly provide the same information. Actually these two methods, though both widely used to determine the LCST of a thermosensitive polymer, provide complementary information by probing two different stages in the phase-transition process at the LCST. Based on this assumption, we put forward a new model to describe the LCST phenomenon in both conventional and phase-separated thermoresponsive hydrogels (Figure 3.9). In the LCST profiles obtained through the cloud point method, the initial transmittance of the three gels are higher than the light transmittance values reported in Table 3.1. Very thin strips of gel were used to measure the cloud point since thick strips would impede uniform heat transfer throughout the sample and thus delay the cloud point.

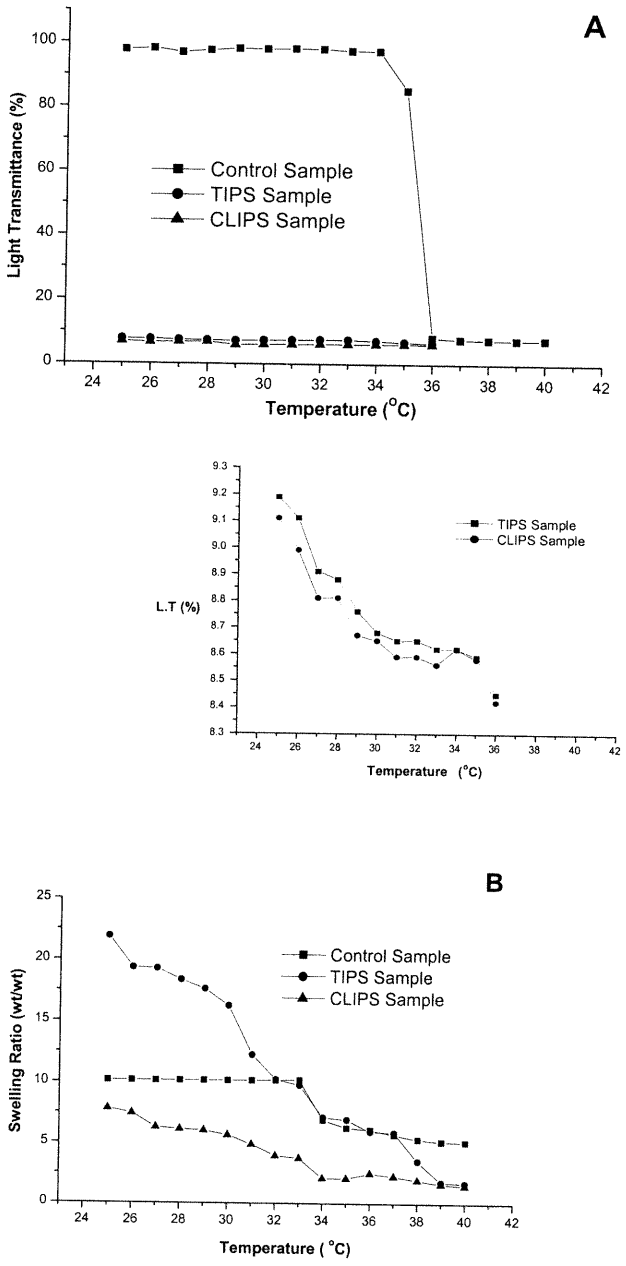

Figure 3.8 Phase-transition profile of conventional and porous thermoresponsive hydrogels using (A) spectrophotometric (transmittance at 600 nm) and (B) gravimetric techniques. Sample composition - Control sample: DEA - 0.2 g, MBA - 0.01 g, APS – 0.002 g; TIPS sample: DEA – 0.2 g. MBA – 0.01 g, APS – 0.002 g; (reaction conditions: 10 minutes above LCST, remainder at room temperature). CLIPS sample: DEA - 0.2 g, MBA - 0.01 g, APS - 0.002 g.

The profile for the conventional gel follows the classical inverted S-curve. At a certain temperature, corresponding to the LCST (34°C), we see an abrupt decline in the transmittance, which corresponds to the cloud point. Both phase-separated hydrogels, though already opaque, show a slight decline in light transmittance. A loss of transmittance signal for both the phase-separated hydrogels was observed at 36°C. This was observed to be due to a drastic loss of mass at this temperature which caused the gel to rise to the water surface.

This light transmittance experiment has revealed two important observations concerning phase-separated hydrogels: (a) there is a small change in opacity in the case of phase-separated gels, and (b) there is an abrupt loss of signal at 36°C.

This abrupt change in size led us to monitor the change in swelling ratio of the three hydrogels as a function of temperature. The weight change profile presents a different picture. The profile of the conventional hydrogel does not vary as dramatically as that of the porous hydrogels. The heating regime was different in both cases – for the cloud point measurements, the gels were subjected to a heating rate of 1°C/min, whereas for the gravimetric method, the gels were made to equilibrate for half an hour at each temperature, before the weight was recorded. Thus, while we should not attempt to compare the LCST obtained using both methods, our focus will be to compare the phase transition profile of conventional gels with that of phase-separated gels for each method.

With the gravimetric method, in the case of conventional gels, one observes the same discontinuous change in weight as was the case with light transmittance. On the other hand, the profile for both phase-separated hydrogels differs substantially from the profile obtained through spectrophotometry. Unlike the profile for the conventional gel, both phase-separated hydrogels undergo steep but continuous decrease in weight till they lose upto 90% of their original weight. It can be seen that there is no single temperature at which the phase-separated gel undergoes a transition. Rather we observe a temperature range (27°C-34°C) at which there is a steeper decline in weight. This stands in contrast to the phase transition profile of the conventional gel where we see an discontinuous change in weight at a single critical temperature (34°C).

All the above observations indicate that the mechanism of phase-separation differs substantially from that of conventional hydrogels. These observations have been used to construct a simple qualitative model to describe the LCST phenomenon in both conventional and porous hydrogels. This model is illustrated in Figure 3.9.

For the model, the basic premise is that the phase transition process in thermoresponsive hydrogels is a two-step process. Heating the gel to the LCST causes the polymer chains to aggregate. Once these aggregates reach a critical size, comparable to the wavelength of light, they scatter light, which causes the gel to turn opaque. Thus the cloud point indicates the appearance of hydrophobic microdomains of a critical size. Very little water is expelled during this process. Further heating causes these domains to coalesce. Once they reach a critical size, they would shrink, thus expelling a large quantity of water. The latter corresponds to the abrupt decrease in the swelling ratio of the hydrogel. Therefore, the spectrophotometric technique and the gravimetric technique are two complementary methods that probe two distinct stages of the phase transition process in thermosensitive hydrogels.

In the case of phase-separated hydrogels, the mechanism is quite different. In this case, the hydrogel is already phase-separated and thus already opaque. The slight increase in the cloud point corresponds to the growth of the already existing domains. According to established theories in colloidal chemistry, light scattering in a medium is dependent both on the number of aggregates and their size. The coming together of large hydrophobic aggregates facilitates the expulsion of water. It is quite evident that large aggregates and short distances between them would favor contraction and, hence, expulsion of water. Thus, these hydrogels expel a large amount of water and shrink drastically to form a more compact mass.

In our efforts to "measure" the thermal response of a hydrogel, we have introduced a new parameter called the *shrinking capacity*. The shrinking capacity of a thermosensitive hydrogel is a measure of the water expelled at a certain temperature above the LCST. Since we have monitored the deswelling/recovery profile of both conventional and phase-separated hydrogels at 50°C, we shall determine the shrinking capacity at the same temperature

(a)

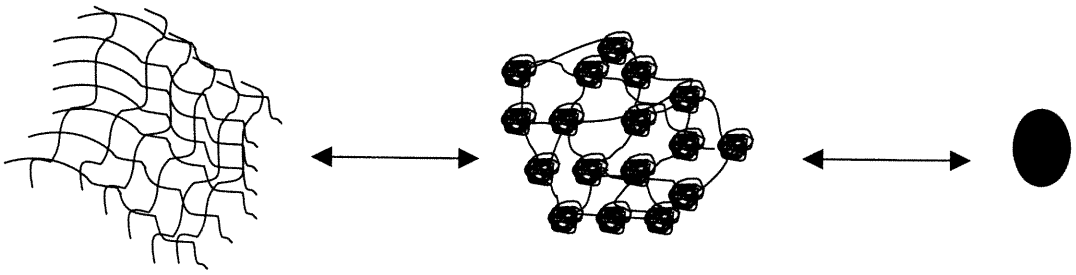

Homogeneous Network

Cloud point corresponding to formation of microaggregates of critical size. Slight expulsion of water

Collapse of gel followed by expulsion of water

(b)

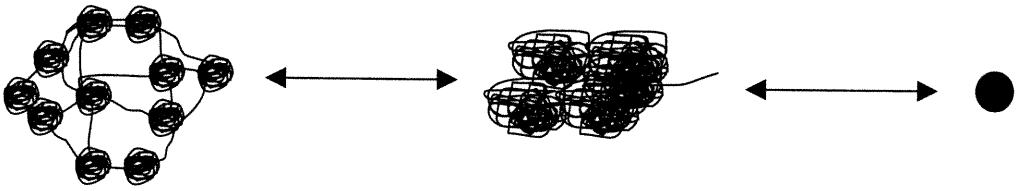

Heterogenous Porous Network

Conglomeration of existing aggregates. Large expulsion of water.

Collapse of gel followed by almost total expulsion of water

Figure 3.9 Conceptual model of the LCST phenomenon in (a) conventional and (b) porous thermoresponsive hydrogels.

We define shrinking capacity (C_{sh}) as

$$C_{sh} = \frac{W_{sw} - W_{sh}}{W_{sw} - W_d} \times 100$$

where W_{sw} is the swollen weight at equilibrium, W_{sh} the shrunk weight at a given temperature above the LCST, and W_d the dry weight. (W_{sw} - W_{sh}) corresponds to the amount of water expelled above the LCST, while (W_{sw} - W_d) corresponds to the total water content in the gel.

Thus the shrinking capacity is a parameter that quantifies the "thermosensitivity" of the hydrogel, i.e., it is a measure of the amount of water a thermoresponsive hydrogel can expel at a critical temperature. In general, the shrinking capacity can be likened to the "actuating power" of a stimuli-responsive hydrogel.

3.2.2 Profile of Deswelling–Recovery Kinetics

As mentioned earlier, one of the key incentives to prepare porous hydrogels was to improve their swelling kinetics. Most of the potential applications of thermosensitive hydrogels involve a temperature-cycling process, i.e., absorption of water along with dissolved solutes at low temperatures followed by its release at higher temperatures. To test the efficiency of shrinking and recovery, we studied the deswelling kinetics profile at 50°C, followed by reswelling at room temperature (25°C). The profiles for the conventional and phase-separated hydrogels are illustrated in Figure 3.10.

As expected, both phase-separated hydrogels drastically shrink and attain a constant weight in about 15 minutes. On the other hand, the conventional gel barely expels 33% of its water in the same time period. This has already been described in the previous section. Porous hydrogels, being already phase-separated at the supramolecular level, contain hydrophobic microaggregates that are able to coalesce into a small compact mass above the LCST, thus expelling a large quantity of water.

The deswelling kinetics profile follows a first order exponential decay for both the phase-separated gels (Appendix- II). A similar dehydration kinetics profile was obtained by Gotoh *et al.* [64], though no curve-fitting was carried out. We were unable to obtain fits for the recovery curve as the gel was not allowed to reach the equilibrium swelling ratio.

From this graph, it is obvious that for application purposes, it would be far more advantageous to use temperature-induced phase-separated gels as they have both a large swelling and a large shrinking capacity.

Thus the shrinking capacity for the three hydrogels at 50°C are as follows:

- Temperature-induced phase-separated gel : 94.7 %
- Crosslinking induced phase-separated gel : 81.3 %
- Conventional gel : 31.6%

It is evident from the data above that the shrinking capacities of the phase-separated gels are far higher than those of conventional gels.

The recovery kinetics of these three gels presents a totally different picture. Here we find that that phase-separated gels are the slowest to recover. None of the gels are able to reach their equilibrium swelling values within the first hour. From Figure 3.9, it is apparent that such a behavior fits in with the model. It is obvious that the smaller and more compact the shrunk gel (as is the case with phase-separated gels), the longer it will take for the polymer chains to relax and reach their equilibrium swelling ratio - hence the slow recovery kinetics of the phase-separated gels as compared to the conventional gels.

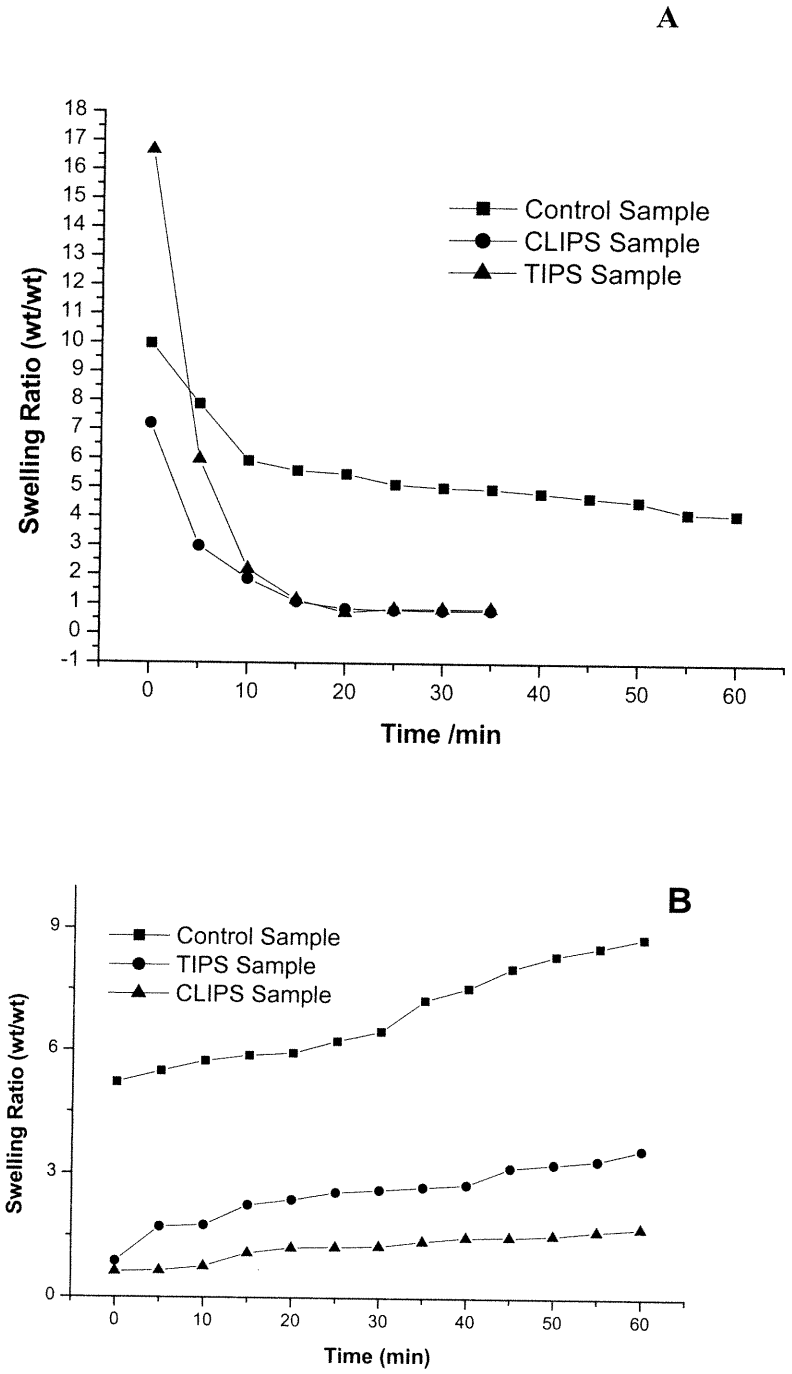

Figure 3.10 Deswelling (Graph A) and recovery (Graph B) kinetics profile of conventional versus porous thermoresponsive hydrogels. Gel composition - Control sample: DEA - 0.2 g, MBA - 0.01 g, APS – 0.002 g; TIPS sample: DEA – 0.2 g. MBA – 0.01 g, APS – 0.002 g; (reaction conditions: 10 minutes above LCST, remainder at room temperature). CLIPS sample: DEA - 0.2 g, MBA - 0.01 g, APS - 0.002 g.

It would be useful at this stage to compare the results obtained here with those already published in the literature. Almost all the research groups working on porous thermoresponsive hydrogels reported the same asymmetric swelling/shrinking behavior, i.e., fast shrinking and slow recovery, as we observed. In all cases, the shrinking rate was much higher than the swelling rate. Gotoh *et al.* [64] produced heat transfer curves for both conventional and phase-separated gels to show that the rate of heat transfer was much higher in the case of phase-separated gels – hence the fast shrinking kinetics. Wu *et al.* [60] also pointed to the asymmetric shrinking/swelling kinetics behavior, as did Kabra *et al.* [62]. We noticed that the shrinking and swelling kinetics of their gels was much faster than that of our gels. This could be because the gels they used were much smaller – 20 mm diameter disks, compared to the 5 cm disks that we used. Moreover, they used disks whose surface had been cut, thus exposing the pores. The gels used in this study were removed straight from their mold and analyzed without any further cutting of the sample.

3.3 Effect of Drying Methods on Water Absorption Kinetics and Morphology

One of the main drawbacks of conventional gels is the slow water uptake kinetics for the dry gel to reach a fully swollen gel. This is a serious impediment to developing viable gel-based absorbents or actuators. We believe that drying methods play a vital role in the swelling kinetics. According to studies on inorganic sol-gel materials, it was reported that conventional oven-drying methods cause the pores in the gel to collapse. It was shown that supercritical drying would preserve the pores [78]. It is a method whereby the sample is brought to a certain critical temperature and pressure where the liquid in the pores vaporizes and leaves the gel without causing a collapse of the pores. However, it is unlikely that a hydrogel would withstand such conditions. Thus, other drying methods have been explored.

We thus decided to compare three simple drying methods – (i) oven drying, (ii) solvent exchange with a more volatile solvent (acetone) followed by oven drying, and finally (iii) freeze-drying. The effect of these three drying methods on the

swelling kinetics and the microstructure is shown in Figures 3.11 and 3.12, respectively.

A significant change in morphology can be observed. In fact, a difference in appearance and texture was easily noticed. Both the oven-dried gel and the gel dried through solvent exchange followed by evaporation were transparent and possessed a hard glassy texture. The freeze-dried gel was opaque and had a soft texture resembling that of Styrofoam. As mentioned earlier, an opaque appearance suggests the formation of discrete domains capable of scattering light. Indeed, as the images show, the one corresponding to the freeze-dried gel reveals a cellular morphology, usually associated with porous structures. The image also shows the presence of what looks like channels which probably allows for the flow of solvent throughout the gel matrix. This would also explain why this gel is able to absorb more water in a shorter period of time than its conventional counterparts.

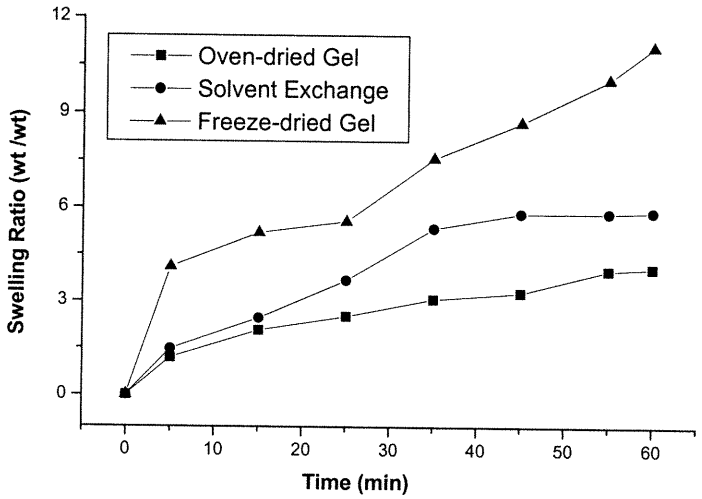

Figure 3.11 Influence of drying methods on swelling kinetics of dry gel. Sample composition: 0.2 g DEA, 0.006 g MBA, 0.002 g APS. (a) Sample dried in conventional oven. (b) Sample dried through solvent exchange with acetone followed by drying in oven. (c) Sample dried through freeze-drying.

It is interesting to note that the opacity of the freeze-dried gel disappears on being swollen in water. This suggests that whatever inhomogeneities that were created during the freeze-drying process were temporary and are lost on rehydration. Thus, freeze-drying as a technique is not suitable for creating permanently porous materials.

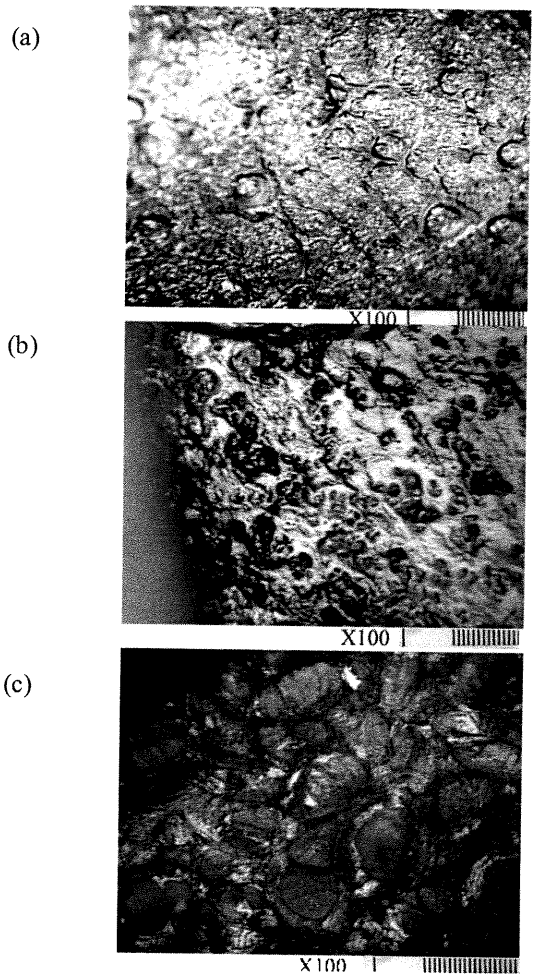

Figure 3.12 Influence of drying methods on gel microstructure. Images obtained through inverted optical microscopy. Sample composition: 0.2 g DEA, 0.006 g MBA, 0.002 g APS. (a) Sample dried in conventional oven. (b) Sample dried through solvent exchange with acetone followed by drying in oven. (c) Sample dried through freeze-drying. One can discern the appearance of small channels around islet-like structures in the case of (c). Each division on the scale corresponds to 10 μm.

The gel dried through solvent exchange with acetone followed by evaporation shows a moderate increase in water uptake kinetics. This could be attributed to the fact that the gel does not aggregate as acetone is being expelled, i.e., the LCST type behaviour that occurs with water is not observed in the case of acetone. Thus, it swells slightly more. The images show a different topography, though it would be difficult to extract any further information. Thus, drying methods do influence the microstructure and hence the swelling kinetics of the gel. It is a point worth considering when preparing gels for absorbent/release applications.

3.4 Influence of Other Synthesis Variables

During the course of this study, it was noted that a few other factors also influenced the microstructure of the hydrogel. For example, it was observed that a change in mould geometry caused a change in turbidity of the sample. Generally, the same reaction mixture, when poured into a narrower mould (ex: a 1-cm diameter culture tube rather than a 6-cm glass vial) became more turbid on gelation. This suggests that narrow moulds facilitate phase separation. Further studies have to be done to confirm these findings. Furthermore, the addition of excess TEMED caused the reaction mixture to instantly gel and turn opaque. Moreover, if the gelation was carried out in long tubes (approximately 12 cm long with a diameter of 1 cm) , the rate of gelation was faster than the rate of diffusion of TEMED throughout the reaction mixture. As a result, we were able to obtain gels with a pore gradient. In other words, we obtained a gel cylinder whose opacity diminished as a function of depth. These are precisely the kind of gels that have been used to demonstrate various potential applications of porous thermoresponsive hydrogels.

3.5 Potential Applications of Porous Thermoresponsive Hydrogels

The unique phase transition behavior of porous thermoresponsive hydrogels was exploited to create models of shape-memory materials and artificial muscles. To do so, we will first explain the method used to create thermoresponsive hydrogels with a pore gradient. Figure 3.13 illustrates the mechanism described below.

3.5.1 Synthesis of Thermoresponsive Hydrogels with a Pore Gradient

As mentioned in the previous section, the addition of TEMED causes the pre-gel solution and hence the gel to turn opaque. This suggests that, like temperature and crosslinker concentration, the TEMED concentration also plays a role in creating porous structures. Here two explanations are possible. It is known that TEMED causes the decomposition of the initiator, accompanied by a large amount of heat. It could well be that the heat produced raises the temperature of the gel solution to above the LCST, hence causing microphase separation. Alternatively, if the same solution was allowed to gel in the refrigerator at 10°C, the opacity diminished gradually, hence confirming the effect of heat, produced by TEMED, on phase separation. However, in a parallel experiment, we found that gelling a solution of acrylamide along with MBA as a crosslinker in the presence of TEMED also produced an opaque gel. Polyacrylamide, as we know, is not thermosensitive and does not possess an LCST. Thus, heat is not necessarily the only factor in creating phase-separates structures using TEMED. Another possible explanation could be that TEMED accelerates the gelation reaction to such an extent that it causes the freezing-in of aggregates through rapid crosslinking, thus leading to a heterogeneous structure with areas rich and sparse in polymer domains.

When a few drops of TEMED (10 μl TEMED for a 2 ml gel solution) are added to the pre-gel reaction mixture in a cylindrical tube, the top portion of the reaction mixture is the first to come in contact with TEMED. Since the gelation reaction with TEMED is almost instantaneous, the top portion consumes a significant amount of the accelerator thus gelling into an opaque mass. This leaves a smaller amount of TEMED to permeate downwards and cause gelation. Thus, the layer in the middle would be less opaque and hence less porous than the layer at the top. This leaves virtually no TEMED left for the bottom section of the tube. Thus the portion of the gel formed in this region is almost transparent. In this manner, we were able to produce a gel with a pore gradient. Such gels form the basis of two potential applications of porous thermoresponsive hydrogels discussed below.

3.5.2 Thermoresponsive Shape-Memory Hydrogels

To create shape-memory materials, the pre-gel reaction mixture was poured into a test-tube, the mixture was then degassed and sealed. Thereafter, a few drops of TEMED (10 μl TEMED for a 2 ml gel solution) were introduced into the solution. The reaction mixture gelled within two minutes with the top portion of the gel totally

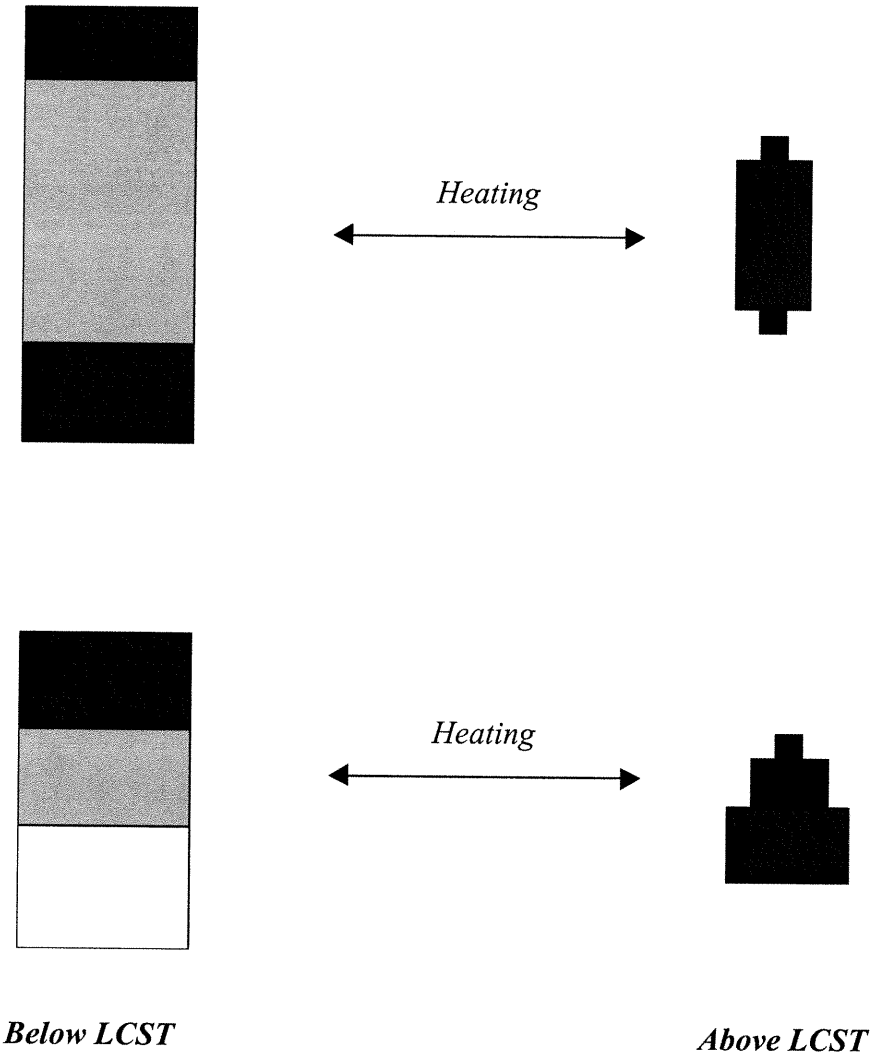

Figure 3.13 Working model of thermoresponsive hydrogels with pore gradient as shape-memory materials (SMM). When the temperature of the gel is raised to a temperature above the LCST, the cylindrical structure shrinks with the more opaque regions (more porous) undergoing a larger collapse ratio than the transparent portions (less porous). Thus a unique shape is obtained in each of the two cases with the gel recovering its original conformation upon cooling.

opaque and the bottom portion totally transparent. On allowing the reaction to proceed towards completion, a gradient was formed. We could see a clear transition from an opaque section to cloudy to almost transparent. The shrinking of this gel was quite spectacular (Figure 3.13). On heating the gel to above its LCST, the opaque portions, being porous, shrank much more than the other more transparent section. Thus the cylindrical gel assumed a more conical shape. It was able to recover its original cylindrical shape on cooling.

3.5.3 Thermoresponsive Gel Actuators: Model of an "Artificial Muscle"

To demonstrate the potential use of a thermoresponsive hydrogel as an artificial muscle, we synthesized a hydrogel cylinder with the one end opaque and the other end transparent. To do so, the gel mixture was allowed to gelate with one end immersed in an oil bath maintained at 40°C (above the LCST). This gel was then immersed in a water bath with the transparent end gently clamped and the opaque end pointing downwards. When the temperature of the water was raised to above the LCST, the porous end once again shrunk more than the non-porous end. Being much lighter, the porous end was inclined to move towards the surface of the water, but was prevented from doing by the clamp. Thus, the contraction was followed by the bending of the gel as the porous end tried to move upwards, thus simulating the elementary movement of a muscle.

Similarly, we demonstrated the use of thermoresponsive hydrogels with a pore gradient, as a tweezer or "finger" to trap fragile objects under water. In this case, we synthesized a thermoresponsive hydrogel with both ends opaque and the middle section transparent. To do so, we allowed the solution to gelate in a tube with one end of the cylinder immersed in an oil bath maintained at 40°C. At the same time, we added two drops of TEMED to the surface of the solution to induce phase separation at the top. This gel was then suspended in water, with its two porous ends hanging parallel to each other. On heating the solution, the gel shrank in a non-uniform manner. The opaque ends shrank much more than the middle section (Figure 3.14). Again, the two ends were inclined to move towards the surface. In trying to do so, these two ends came close to each other. Such a position would allow for picking up

of a light object under water. This is the working principle of a chemomechanical system or a gel "tweezer". What is remarkable about this system is the ability of a gel to grab an object as well as raising the object towards the surface of the water. We would, however, need to work on improving its mechanical properties.

An important point worth mentioning here is the direction of the bending of the gel. While a gel with a pore gradient shows a clear deflection above the LCST, one needs to also consider the direction of bending. One way of possibly controlling the direction could be to vary the initial inclination of the gel cylinder to favor one direction over another. This is an area that would have to be developed.

Similar work on gel-based artificial muscles has been conducted by Zhibing Hu *et al.* [79]. His research group has also been working on gels whose composition is engineered so that, in response to a specific stimulus, they spontaneously bend or curl into a predetermined shape.

Hu and his coworkers have prepared gels that have a heterogeneous or modulated structure. They used two polymers with different sensitivities, such as PNIPAM and polyacrylamide. The gels are synthesized side-by-side in sequence in such a way that a part of one gel's network interpenetrates the other gel's network. In other words, across the thickness of the gel, its composition changes gradually from pure polyacrylamide, to a mixture of polyacrylamide and PNIPAM, to pure PNIPAM. Using this method, the researchers have fabricated bigel strips in which slabs of the two different polymers are intergrown together. The two polymers respond differently: PNIPAM shrinks drastically when warmed above 37°C, whereas the polyacrylamide gel does not. The polyacrylamide gel, however, shrinks much more than the PNIPAM gel when the acetone concentration of the aqueous medium increases beyond 34%. Thus, by choosing the appropriate temperature and solvent conditions, the bigel strip can be made to bend into a "C" with either one polymer or the other inside the arc. The shape changes are reversible. Thus they were able to control the direction of shrinkage. We can foresee a variety of applications for such

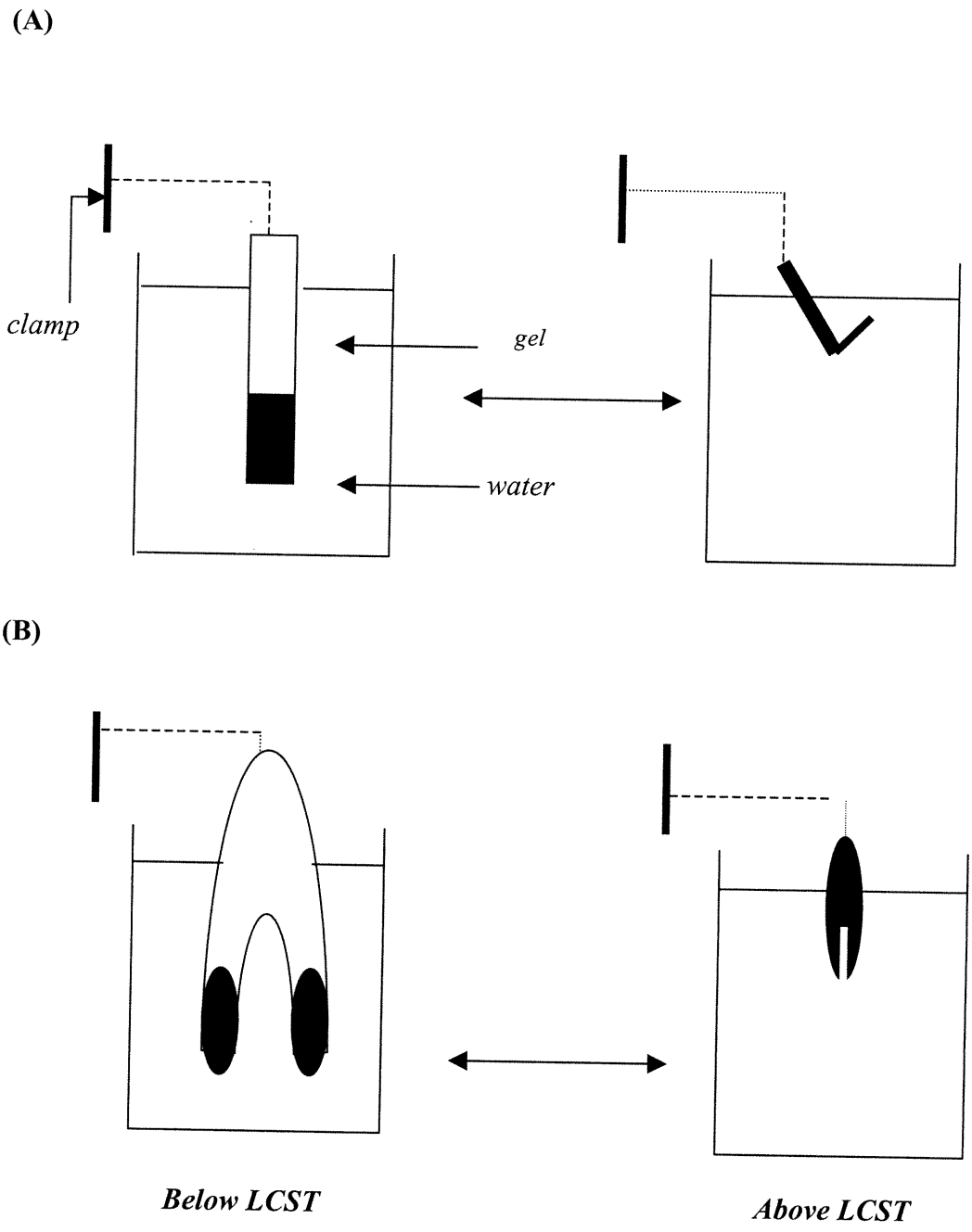

Figure 3.14 Working model of thermoresponsive hydrogels with pore gradient as chemomechanical systems. (A) "Artificial muscle": Heating above the LCST causes the gel to shrink and bend with lighter porous sections (opaque region) moving towards the surface. (B) Gel "finger": On heating above LCST, porous ends shrink and come together thus displaying a finger like motion. Direction of shrinkage largely depends on the ratio of the opaque portions to the transparent portions as well as the initial direction of inclination.

shape-memory materials. One could design thermosensitive soft tweezers to trap and release fragile material. Such devices could have environmental and surgical applications Furthermore, one could prepare injectable biomaterials by pouring a gel solution on to a site and then carrying out in-situ polymerization using light or heat. Using the same principle, we can create a pore gradient by subjecting certain areas to more radiation (higher temperatures) than others, and thus molding the gel into a certain shape suitable for various biomedical applications. Other potential application could include bendable surgical tools, flexible medical devices such as catheters and stents.

Thermosensitive hydrogels with a pore gradient could also be used as a separation medium in gel permeation chromatography or gel electrophoresis. Other potential applications of porous thermoresponsive hydrogels are discussed in Chapter 4.

It must be noted that further developments in the field of gel actuators would involve developing a mathematical framework to evaluate their performance. While shrinking capacity is in fact a measure of the actuating power of the artificial muscle, their exist other parameters and measurements used in physiology to characterize muscles. Such parameters could be used to characterize the actuating capacity of artificial muscles. Details of the same are elaborated upon in Section 4.3.6.

4. Summary and Conclusions

The present study has contributed to our understanding of the physicochemistry of porous thermoresponsive hydrogels and the effect of gel morphology on their swelling and thermoresponsive behavior. The peculiar phase-transition behavior of thermoresponsive hydrogels also led us to design hydrogel-based shape-memory materials and chemomechanical systems. This chapter provides a brief overview of the results obtained as well as a discussion of the significance of this work.

4.1 Summary of Results

4.1.1 Influence of Microsyneresis on Microstructure and Water Absorption.

We have shown that both temperature and crosslinking can induce microphase separation which creates porous structures in thermoresponsive hydrogels. The water absorption capacity of the porous gels synthesized through TIPS was higher than that of conventional gel, while those obtained through CLIPS exhibited lower swelling ratios than those of conventional gels. This is attributed to the creation of wide water channels in the case of TIPS gel which allows for free flow of water throughout the sample. The porous hydrogels obtained through CLIPS contain water islets trapped in a largely hydrophobic matrix with only a few interconnected pores. This study demonstrated the ease with which one could obtain thermoresponsive hydrogels with the desired swelling ratio, porosity and texture by simply modulating the synthesis conditions.

The microscopic images obtained show clearly the presence of pores in the size of approximately 10 - 20 μm in phase-separated hydrogels. We could also see a transition from a percolated morphology to a droplet morphology on increasing the cross-linker concentration.

Optical microscopy provides details of both of the extent of heterogeneity in a system, the average pore size, as well as the nature of the pores. The obvious advantage of this method is that the sample does not have to undergo any preliminary treatment, unlike scanning electron microscopy, that might modify the

microstructure. The optical images provided us with basic information on porosity and allowed us to see whether the nature of the pores be it interconnected or isolated.

4.1.2 Phase Transition Behaviour of Porous Hydrogels versus Conventional Hydrogels

We have probed the thermosensitive behavior of phase-segregated hydrogels. Our original assumption was that such thermosensitive hydrogels, where the lateral hydrophobic chains are already aggregated, would not undergo any further aggregation. Hence, it was assumed that these hydrogels would not display any thermosensitive behavior. Gravimetric measurements presented a different picture. The phase-separated gels shrink far more rapidly than conventional gels expelling up to 95% of its water at temperatures as low as 50°C. This is a useful property for reversible absorbents or recovery of certain specific solutes from aqueous media. This abrupt volume change can also be translated into a force and be used as a chemomechanical system. This ability to expel large amounts of water at its LCST was also manifested by favorable deswelling kinetics. However, we noticed that the same features that contributed to fast dehydration kinetics were also the cause for slow water recovery kinetics. The phase-segregated hydrogel formed a tight, compact mass on shrinking and took much longer for the aggregates to recover their original conformation. Based on these observations, we conceived a model to describe the LCST phenomenon in both conventional and porous hydrogels. What distinguishes our model from the others is the fact that we have examined the phase-transition as a two-step process involving first the formation of microaggregates followed by the coalescence of these microaggregates into a compact globule.

4.1.3 Influence of other Synthesis Variables on Hydrogel Properties

We have highlighted the significance of drying methods both on gel morphology and swelling kinetics – a point that has been mentioned only cursorily in the literature. We have confirmed that freeze-drying indeed creates a porous structure but have observed that this morphology disappears when swollen to equilibrium,

thereby suggesting that the pores created are temporary. This proves that permanent morphological features can be created only during the actual gelation process, be it foaming, phase separation or porogen methods. This is a point that should be taken into account when designing fast-response hydrogels.

4.1.4 Potential Applications of Porous Thermoresponsive Hydrogels

We have demonstrated the potential applications of porous thermoresponsive hydrogels as shape-memory materials and artificial muscles. Their use as shape-memory materials is based on the differences in shrinking capacities between porous and conventional gels. By varying the microstructure at different points along the length of a gel cylinder, we have created structures that respond differently at different portions to a temperature stimulus. Hence, they assume a unique shape on heating and recover their original shape on cooling.

We have also demonstrated the viability of thermoresponsive hydrogels as reversible absorbent materials for the recovery and release of water-soluble substances. Such a property would be useful in drug release and environmental applications.

4.2 Contribution to Original Knowledge

The results obtained here have contributed to a better understanding of porous thermoresponsive hydrogels, while at the same time established a basic framework on which further theoretical and practical aspects can be explored. We have further developed on the work on porous thermoresponsive hydrogels, initiated by S. Gehrke and others. Our work involved a more fundamental approach. Our starting point was a systematic study of the effect of synthesis conditions that lead to microphase separated structures in thermoresponsive hydrogels. This is also the first time that the role of a porous microstructure on the LCST has been investigated. We have also introduced *shrinking capacity* as a parameter to quantify the response of a hydrogel to a thermal, or any other, external stimulus. This is a very useful parameter for it allows

us to compare the response of various stimuli-responsive hydrogels to specific external stimuli. The shrinking capacity would provide valuable information when designing gel-based actuators. Finally, by synthesizing thermoresponsive hydrogels with a pore gradient, we were able to design shape-memory materials and chemomechanical systems that have potential applications in medicine and engineering. This study on porous thermoresponsive hydrogels provides insights into the fascinating chemistry as well as their potential applications.

However, it is clear that there is still work to be done. The following section outlines some of the future directions in the field of thermoresponsive porous hydrogels.

4.3 Future Work

4.3.1 Kinetics of Swelling

One of the main challenges would be to improve the recovery kinetics of collapsed thermosensitive hydrogels. The gels we have designed display the same asymmetric kinetic behavior, i.e., fast deswelling-slow recovery that is often found in the literature. There probably exist certain optimum synthesis conditions that would allow for both fast deswelling and recovery. We would have to vary other synthesis variables like initiator concentration, monomer concentration and temperature, in order to reach an optimum gel composition that would display favorable swelling kinetics. At the same time, this would allow for a better understanding of microphase separation in hydrogels.

4.3.2 Interpenetrating Networks (IPN)

One could experiment with more complex polymer systems or different variations of the same system. One such option to improve swelling kinetics could be based on thermosensitive polymer networks combined with entangled linear hydrophilic chains. Such a system is commonly referred to as a semi-interpenetrating network (semi-IPN), as opposed to an IPN, which consists of two polymer networks

embedded in each other. We could assume that the presence of linear hydrophilic polymers would act as a water channel thus allowing for improved permeation of water throughout the network. Such a gel would probably swell more and faster. Another variation would be to create sequential IPNs based on poly(sodium acrylate) and DEA. We believe that gels based on IPNs would possess better mechanical properties.

4.3.3 Mechanical Properties of Hydrogels

In terms of mechanical properties, high swelling hydrogels can be made more durable by reinforcing them with other materials. One such option could be to create composite hydrogels with silicone-based polymers. This would impart a stronger rubber-like texture to the hydrogel without compromising on its basic hydrophilic character. Another approach could be to create composite gels by combining the thermosensitive polymer network with a poly(vinyl alcohol) solution and then subjecting it to a number of freeze-thaw cycles to create a composite PDEA/PVA hydrogel. The resulting gel would combine both high water uptake and high tensile strength, thus making it suitable for a wide range of applications. It remains to be seen if such polymer gels would retain their thermosensitive properties.

4.3.4 Microsyneresis in Thermoresponsive Hydrogels

The phenomenon of microsyneresis in hydrogels has fascinating theoretical aspects. It is a process worth exploring in detail. We could further develop on the basic temperature-induced microphase separation process by the addition of substances like surfactants or thermosensitive linear polymers during the gelation process. Furthermore, while we have proposed a qualitative model to describe the simultaneous phase separation and gelation, we feel that this could be further improved upon through mathematical models that would relate synthesis variables to the polymer-solvent interaction parameter χ. Such a model would allow for better control of the hydrogel morphology by modulating various synthesis conditions.

Fitting with the Ginzburg-Landau model of spinodal decomposition [79] would reveal other details too. Other variables that are worth examining are the effect of gradual temperature increase and step-wise temperature jumps. The influence of comonomers, whether hydrophilic or hydrophobic, would also be of theoretical and practical interests.

We could also exploit the phenomenon of microphase separation to create phase-separated structures in other hydrogel-based systems. Preliminary experiments in our laboratory have shown that poly(sodium acrylate) gels acquire a heterogeneous phase-separated structure when gelated in the presence of minute amounts of acetone. This is a classic example of a non-solvent-induced phase separation process. We believe that this same principle can be applied to create porous hydrogels for virtually any other polymer.

4.3.5 Analysis of Gel Microstructure

We would also need to concentrate our efforts in developing better microscopic methods to study the microstructure of porous hydrogels. While optical microscopy provides us with basic information on the gel topography, we could extract further information by combining inverted optical microscopy with sophisticated scanning probe microscopy techniques like atomic force microscopy, adhesion force microscopy and so on. By coating the scanning probe tips with hydrophobic molecules, we would be able to determine the hydrophobic/hydrophilic nature of the hydrogel surface, through the extent of adhesion of the tip to the surface. We would also have to develop special cutting methods that would allow probing the interior of the gels without creating artefacts.

4.3.6 Gel Actuators Based on Thermoresponsive Hydrogels

Section 3.7 demonstrated the potential of thermoresponsive porous hydrogels as artificial muscles. Such "artificial muscles" could find applications in robotics, or surgery. However, any viable gel actuator technology would require a mathematical

framework to evaluate its performance as artificial muscles. For this, it would be useful to borrow from biomechanics and muscle physiology and adopt the framework currently used to characterize and study biological muscles. Such measurements include force-length curves, force-velocity relationships and fatigue. The experiments would involve monitoring the contractile behaviour of the hydrogel against a constant load.

4.3.7 Other Potential Applications of Porous Thermoresponsive Hydrogels

Thermosensitive porous hydrogels could be used for many applications in addition to the ones described in Chapter 3. The presence of discrete hydrophobic domains within a hydrophilic matrix could serve as a delivery vehicle for hydrophobic drugs. Such porous structures could also be used as functional scaffolds for tissue regeneration. Porous thermosensitive hydrogels could even find applications in nanotechnology. There are a few research groups working on matrices that could serve as nanostructured environments to grow nanoparticles. In one such study, microphase-separated diblock copolymers have been used as an ordered matrix for the synthesis of palladium nanoparticles [80]. It would be worthwhile to explore the feasibility of thermosenstive porous hydrogels for similar applications, seeing that they have the added advantage of modulating the domain size through temperature change.

It should be emphasized that further developments in this field, both theoretical and practical, would increasingly demand a more cross-disciplinary approach by borrowing on ideas from other areas of research. Many of the ideas for this thesis came from surveying literature on sol-gel chemistry, gel electrophoresis, methacrylate-based polymers, rubbers, biopolymers and even porous geological structures. It is only through such a cross-fertilization of ideas that we could gain deeper insights into the behavior of these fascinating materials and be able to better exploit their unusual properties, whether in traditional applications such as absorbent materials or in cutting-edge fields like nanotechnology and tissue engineering.

References

1. Vincent, J. F. V. *Smart Materials and Structures* **2000**, *9*, 255.
2. Furuya, Y.; Tani, J. *Materials Science Forum* **2000**, *327*, 91.
3. *Optics and Photonics News* **1998**, *9*, 8.
4. Annaka, M.; Tokita, M.; Tanaka, T.; Tanaka, S.; Nakahira, T. *J. Chem. Phys.* **2000**, *112*, 471.
5. Ichijo, H. *et al. Radiat. Phys. Chem.* **1995**, *46*, 185.
6. Mun, C. A.; Nurkeeva, Z. S.; Ermukhambetova, B. B.; Nam, I. K.; Kan, V. A. *Polymers for Advanced Technologies* **1999**, *10*, 151.
7. Choi, O. S.; Yuk, S. H.; Lee, H. B.; Jhon, M. S. *J. Appl. Polym. Sci.* **1994**, *51*, 375.
8. Zrinyi, M. *Colloid Polym. Sci.* **2000**, *278*, 98.
9. Miyata, T.; Asami, N.; Uragami, T. *Nature* **1999**, *399*, 766.
10. Morohashi, S.; Takaoka, M.; Yokoyama, N.; Akakabe, S.; Hoshino, K. *J. Chem. Engn. Jpn.* **2001**, *34*, 430.
11. Dagani, R. *Chem. Eng. News* **1997**, *75,* 26.
12. Ma, J. T.; Liu, L. R.; Yang, X. J.; Yao, K. D. *J. Appl. Polym. Sci.* **1995**, *56*, 73.
13. Markland, P.; Zhang, Y.; Amidon, G. L.; Yang, V. C. *J. Biomed. Mater. Res.* **1999**, *47*, 595.
14. Obaidat, A. A.; Park, K. *Biomaterials*, **1997**, *18,* 801.
15. Osada, Y.; Matsuda, A. *Nature*, **1995**, *376*, 219.
16. Kim, C. *Chemtech*, **1994**, *24*, 36.
17. Kim, J. J.; Park, K. *Bioseparation – Intl. J. Separ. Sci. Biotech.* **1997**, *7*, 77.
18. Schild, H.G. *Prog. Polym. Sci.* **1992**, *17*, 163.
19. Hino, T.; Prauznitz, J.H. *Polym. Commun.* **1998**, *39,* 3279.
20. Badiger, M. V.; Lele, A. K.; Bhalerao, V. S.; Varghese, S.; Mashelkar, R. A. *J. Chem. Phys* **1998**, *109*, 1175.

21. Boutris, C.; Chatzi, E. G.; Kiparissides, C. *Polymer - Letchworth*, **1997**, *38*, 2567.
22. Gundlach, D. P.; Burdett, K. A. *J. Appl. Polym. Sci.* **1994**, *51*, 731.
23. Duracher, D.; Elaissari, A.; Pichot, G. *J. Polym. Sci.,Polym. Chem. Ed.* **1999**, *37*, 1823.
24. Ikehara, T.; Nishi, T.; Hayashi, T. *Polym. J.* **1996**, *28*, 169.
25. Platé, N.A.; Lebedeva, T.; Valuev, L. I. *Polym. J.* **1999**, *31*, 21.
26. Lowe, T. L.; Virtanen, J.; Tenhu, H. *Langmuir* **1999**, *15*, 4259.
27. Sedlakova, Z.; Bouchal, K.; Ilavsky, M. *Polym. Gel Networks* **1998**, *6*, 163.
28. Liu, Y.; Velada, J. L.; Huglin, M. B. *Polymer* **1999**, *40*, 4299.
29. Erbil, C.; Aras, S.; Uyanik, N. *J. Polym. Sci. Polym. Chem. Ed.* **1999**, *37*, 1847.
30. Okazaki, Y.; Ishizuki, K.; Kawauchi, S.; Saton, M.; Komiyama, J. *Macromolecules,* **1996**, *29*, 8391.
31. Mathias, L. J.; Thompson, R.D.; Michalovic, M. *Polym. Commun.* **1998**, *39*, 2693.
32. Byrin, J.; Lee, Y. M.; Cho, C.; Sung, Y. *Kor. Polym. J.* **1995**, *3*, 1.
33. Byrin, J.; Lee, Y. M.; Cho, C.; Sung, Y. *J. Appl. Polym. Sci.* **1996**, *61*, 697.
34. Shin, B. C.; Jhon, M.S.; Lee, H.B.; Yuk, S.H. *Eur. Polym. J.* **1998**, *34*, 171.
35. Zhu, X. X.; Liu, H. Y. *Polymer Preprints* **41**, *998*, 2000.
36. Percot, A.; Lafleur, M.; Zhu, X. X. *Polymer* **2000**, ***41***, 7231.
37. Masaro, L.; Ousalem, M.; Baille, W. E.; Lessard, D.; Zhu, X. X. *Macromolecules* **1999**, *32*, 4375.
38. Percot, A.; Zhu, X. X.; Lafleur, M. *J. Polym. Sci. Polym. Phys. Ed.* **2000**, *38*, 907.
39. Wang, C.; Li, Yong, H.; Hu, Z. *Macromolecules* **1997**, *30*, 4727.
40. Kaneko, Y.; Yoshida, R.; Sakai, K.; Sakurai, Y.; Okano, T. *J. Membr. Sci.* **1995**, *101*, 13.
41. Bae, Y.; Okana, T.; Kim, S. W.; *Pharm. Res.* **1991**, *8*, 531.
42. Lynch, I.; Gorelov, A. V.; Dawson, K. A. *Progr. Colloid Polym. Sci.* **2000**, *115*, 121.

43. Tanaka, T. *Physica* **1986**, *140*, 261.
44. Tanaka, T.; Fillimore, D. J. *J. Chem. Phys.* **1996**, *105,* 4350.
45. Kaneko, Y.; Sakai, K.; Kikuchi, A.; Yoshida, R.; Sakurai, Y.; Okano, T.; *Macromol. Symp.* **1996**, *109,* 41.
46. Haldon, R.; Lee, B. E., *Br. Polym. J.* **1972**, *4*, 491.
47. Kato, N.; Takahashi, F. *Bull. Chem. Society Jpn.* **1999**, *72*, 357.
48. Hu, D. ; Chou, K. *Polym. - Letchworth* **1996**, *37*, 1019.
49. Appel, R.; Xu, W.; Zerda, T. W.; Hu, Z. *Macromolecules* **1998**, *31*, 5071.
50. Chieng, T.; Gan, L. M.; Chew, C. H.; Ng, S. C.; Pey K. L. *Polymer* **1996**, 37, 2801.
51. Righetti, P. G. *J. Chromatogr. A.* **1995**, *698*, 3.
52. Terauchi, K., *J. Appl. Polym. Sci.* **1993**, *50*, 709.
53. *New Materials Japan* **1994**, 15.
54. Okay, O.;*Polymer* **1999**, *40*, 4117.
55. Okay, O :. Durmaz, S. *Polymer* **2000**, *41*, 5729.
56. Chen, J.:Park, H.; Park, K. *J. Biomed. Mater. Res.* **1999**, *44*, 53.
57. Oxley, H. R.; Corkhill, P. H.; Fitton, J. H.; Tighe, B. J. *Biomaterials* **1993**, *14*, 1064.
58. Courtney, J. M.; Murphy, S. M.; Robertson, L. M.; Ryan, C. J.; Tighe, B. J. *J. Biomaterials Sci. Polym. Ed.* **1999**, *10*, 11.
59. Kabra, B. G.; Gehrke, S. H. *Polym. Commun.* **1991,** 32, 322.
60. Wu, X. S.; Hoffman A. S.; Yager, P. *J. Polym. Sci. Polym. Chem.* **1992**, *30*, 2121.
61. Yan, Q.; Hoffman A. S. *Polym. Commun.* **1995**, *36*, 887.
62. Kabra, B. G.; Gehrke, S.H.; Spontak, R.J. *Macromolecules* **1998**, *31*, 2166.
63. Miura T.; Kishi R.; Ichijo H. *Polym. J.* **1999**, *31*, 447.
64. Gotoh, T.; Nakatani, Y.; Sakohara, S. *J. Appl. Polym. Sci.* **1996**, *69*, 895.
65. Kolosov, O.; Suzuki, M.; Yamanaka, K. *J. Appl. Phys.* **1993,** *74*, 6407.
66. Hirokawa, Y.; Jinnai, H.; Nishikawa, Y.; Okamoto, T; Hashimoto, T. *Macromolecules*, **1999**, *32,* 7093.

67. Zhang, W.; Zou, S.; Wang, C.; Zhang, X. *J. Phys. Chem. B* **2000**, *104*, 10258.
68. Kato, N.; Takahashi, F. *Bull. Chem. Soc. Jpn.* **1998**, *71*, 1299.
69. Idziak, I.; Avoce, D.; Lessard, D.; Gravel, D.; Zhu, X. X. *Macromolecules* **1999**, *32*, 1260.
70. Stading, M.; Langton. M.; Hermansson, A. *Makromol. Chem., Macromol. Symp.* **1993**, *76*, 283.
71. Petschek, R.; Metiu H.; *J. Chem. Phys.* **1983**, *79*, 3443.
72. Erukhimovich A., Khokhlov, A.; *Polym. Sci.* **1993**, *35*, 1522.
73. Barry, J. H.; Pant, P.; Wu, F. *Physica - Section A* **1997**, *238*, 149.
74. Dusek, K.; Sedlacek, B. *Czechoslov. Chem. Commun.* **1969**, ***34***, 136.
75. Dusek, K.; Prins, W. *Adv. Polymer Sci.* **1969**, *6*, 1.
76. Gehrke, S.; Fisher J.; Palasis, M.; Lund, M.E. *Annal. New York Acad. Sci.* **1994**, ***179***, 125.
77. Hu, Z. *J. Appl. Polym. Sci.* **1997**, *63*, 1173.
78. Sievers, R.E. *Ind. Eng. Chem. Res.* **2000**, *39*, 12.
79. Nakazawa, H.; Sekimoto, K. *J. Chem. Phys.* **1996**, *104*, 1675.
80. Spatz, J. P.; Eibeck, P.; Mossmer, S.; Moller, M.; Kramarenko, E.; Khalatur, P.; Potemkin, I.; Khokhlov, A.; Winkler, R.; Reineker, P. *Macromolecules* **2000**, *33*, 150.

APPENDIX

Composition of :

Control Sample: 0.2 g PDEA, 0.006 g MBA, 2 ml water

TIPS Sample: Control Sample at 10 minutes above LCST, remainder at room temperature

CLIPS Sample: 0.2 g PDEA. 0.01 g MBA, 2 ml water.

---

1. Data table of Water absorption capacities for PDEA gels as a function of Temperature – Figure 3.9

Temperature / °C	Control Sample	TIPS Sample	CLIPS Sample
25	10.15	21.9	7.81
26	10.14	19.36	7.43
27	10.15	19.28	6.27
28	10.14	18.36	6.12
29	10.15	17.62	6.02
30	10.14	16.25	5.64
31	10.15	12.24	4.88
32	10.15	10.23	3.95
33	10.16	9.76	3.75
34	6.91	7.12	2.09
35	6.26	6.94	2.07
36	6.11	5.96	2.48
37	5.70	5.87	2.24
38	5.31	3.52	1.93
39	5.14	1.76	1.61
40	5.10	1.68	1.48

2. Influence of drying methods on swelling kinetics (Figure 3. 13)

Time/min	Water absorption (wt / wt)		
	Oven- Dried Gel	Solvent exchange	Freeze-dried gel
0	0	0	0
5	1.19	1.47	4.10
15	2.07	2.46	5.20
25	2.52	3.67	5.56
35	3.07	5.34	7.57
45	3.28	5.82	8.7
55	4	5.83	10.05
60	4.07	5.87	11.08

3. Deswelling kinetics of conventional vs porous hydrogels (Figure 3. 12)

Time /min	Swelling Ratio (wt/ wt)		
	Control	CLIPS	TIPS
0	9.97	7.2	16.67
5	7.87	2.98	5.96
10	5.91	1.86	2.19
15	5.58	1.09	1.16
20	5.47	0.85	0.73
25	5.11	0.81	0.85
30	5.01	0.79	0.85
35	4.96	0.79	0.85
40	4.82		
45	4.67		
50	4.54		
55	4.14		
60	4.10		

4. Recovery kinetics of Conventional vs. Porous hydrogels (Figure 3.12)

Time /min	Water absorption (wt / wt)		
	Control Sample	TIPS	CLIPS
0	5.21	0.88	0.63
5	5.49	1.72	0.65
10	5.74	1.76	0.76
15	5.88	2.25	1.09
20	5.94	2.38	1.22
25	6.24	2.56	1.24
30	6.48	2.62	1.26
35	7.25	2.69	1.38
40	7.55	2.75	1.48
45	8.04	3.16	1.49
50	8.35	3.25	1.53
55	8.55	3.34	1.63
60	8.78	3.6	1.71

Dehydration Kinetics of CLIPS and TIPS Samples

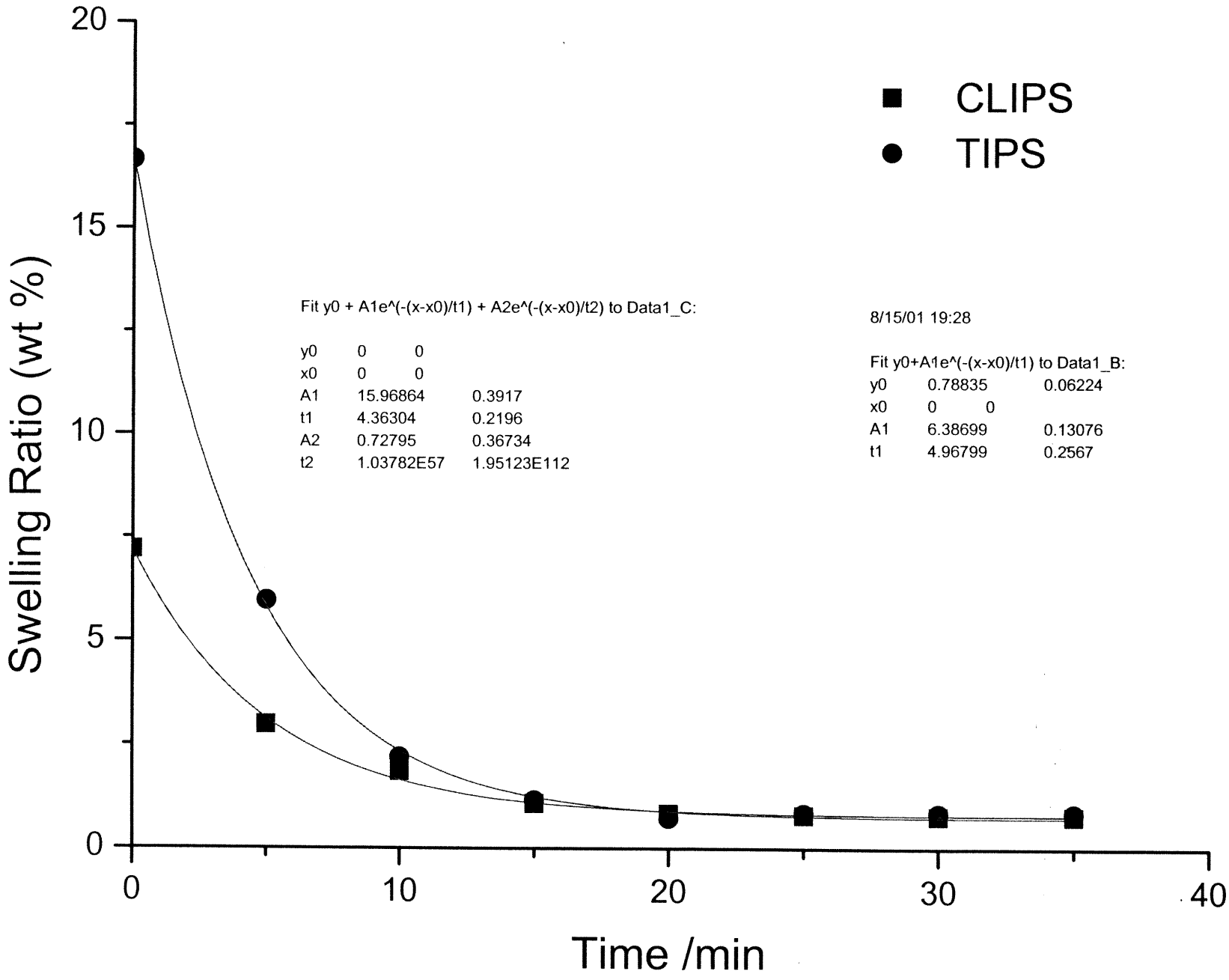

Fit y0 + A1e^(-(x-x0)/t1) + A2e^(-(x-x0)/t2) to Data1_C:

y0	0	0
x0	0	0
A1	15.96864	0.3917
t1	4.36304	0.2196
A2	0.72795	0.36734
t2	1.03782E57	1.95123E112

8/15/01 19:28

Fit y0+A1e^(-(x-x0)/t1) to Data1_B:

y0	0.78835	0.06224
x0	0	0
A1	6.38699	0.13076
t1	4.96799	0.2567